Bridging Input and Evaluation: Leveraging PFISR Data in I-T Modelling Studies

24 July 2025

Doğacan Su Öztürk

dsozturk@alaska.edu

Outline

I. A brief introduction of meso-scale structures.
What are they and why are they important?

II. Leveraging PFISR data to study meso-scale structures.
How can we utilize PFISR data to solve long-known problems in numerical models?

III. Case evaluation and model validation with PFISR data.
How can we utilize the PFISR data to gain better insight on coupled processes across the M-I-T system?

What are meso-scale structures and why are they important?

Large-Scale Processes in the Geospace System

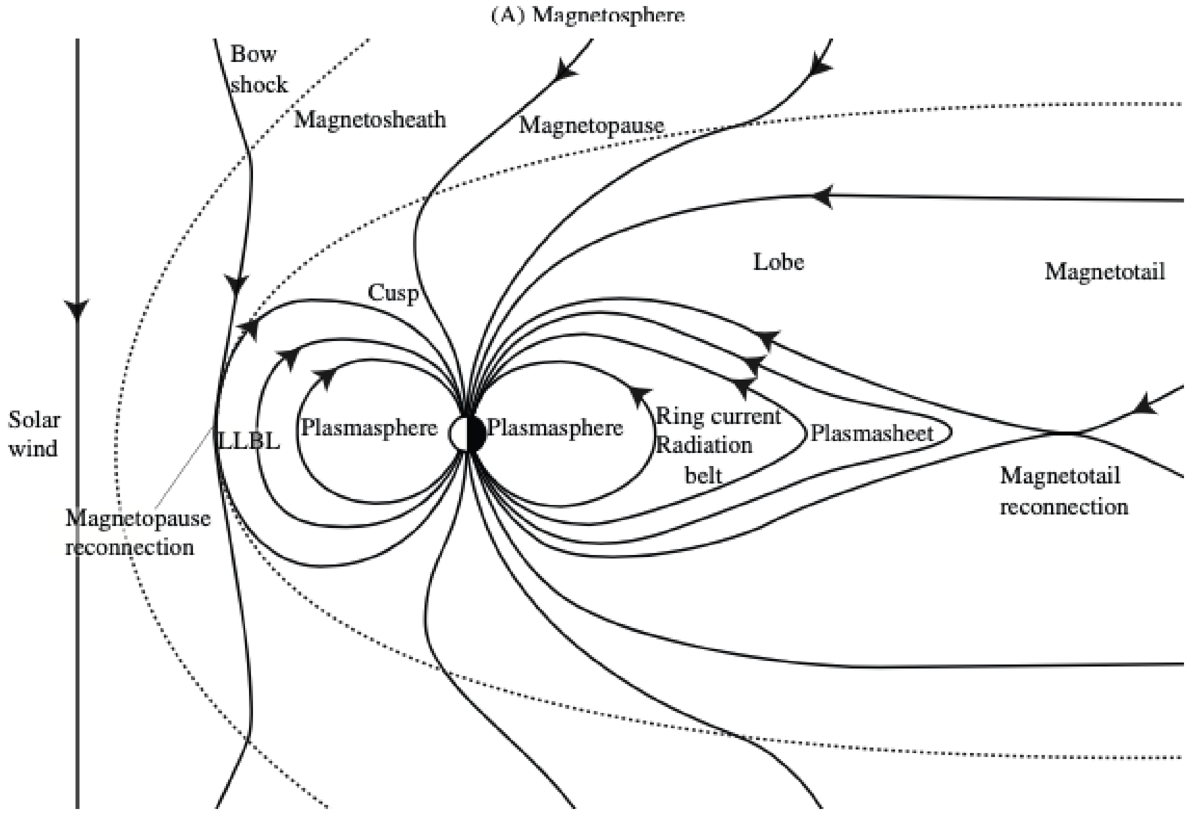

Ionospheric convection – analogous to magnetospheric convection and creates the electric field potentials.

Field-aligned currents – R1 and R2 systems emerging as a result of magnetospheric convection and partial ring current.

Auroral oval – the region of effective precipitation.

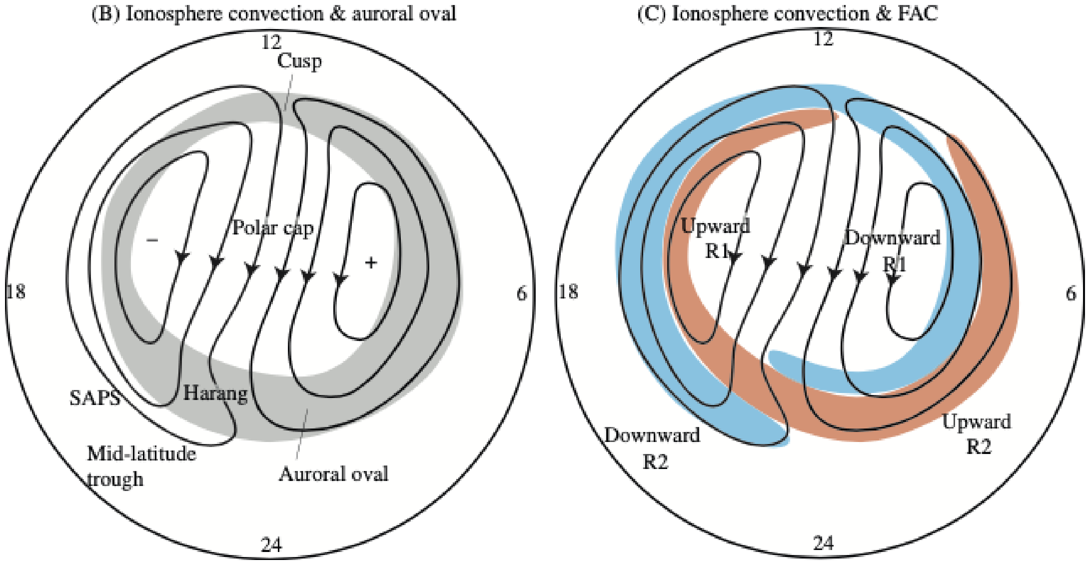

Dungey Cycle describes the interaction of solar wind with planetary magnetosphere. ~ 3 hours

Nishimura et al., 2020

Meso-scale Processes in the Geospace system

Dayside meso-scale processes

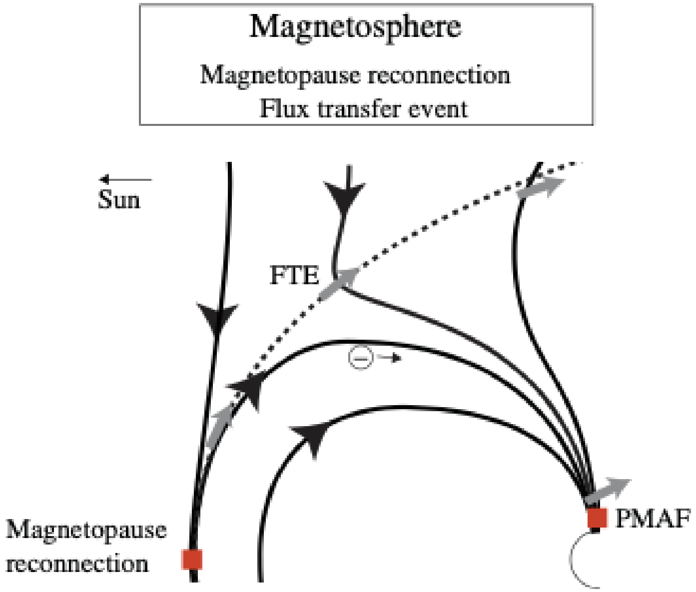

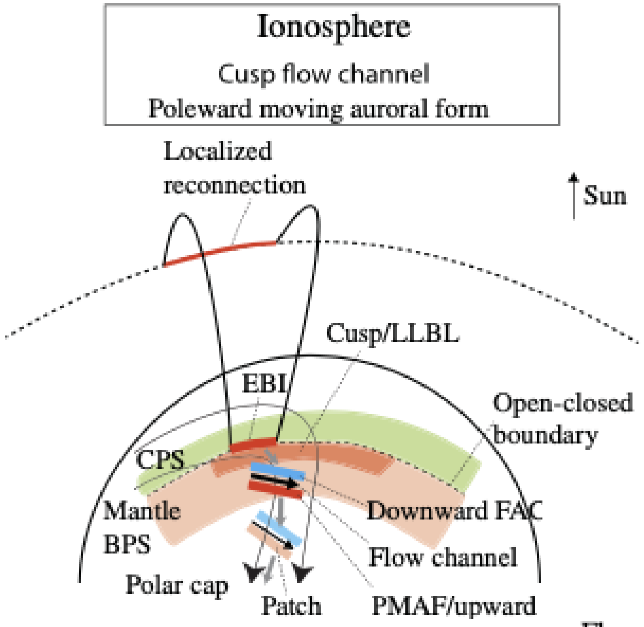

Localized, dynamic structures with temporal scales of **2-15 minutes** and spatial scales of **100-500 kms**.

Can demonstrate characteristics **as intense as large-scale** structures.

Nightside meso-scale processes

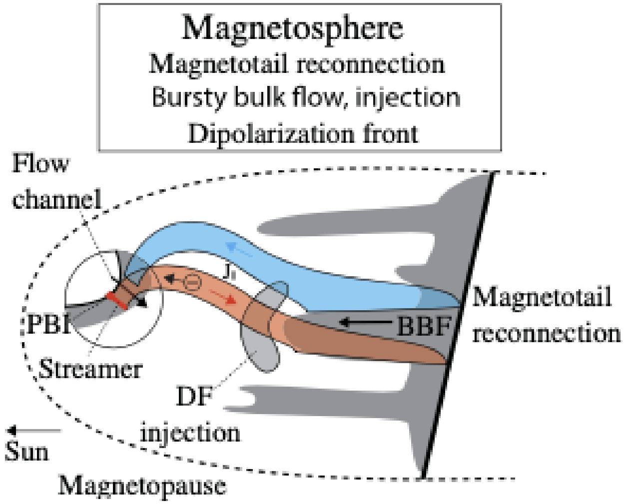

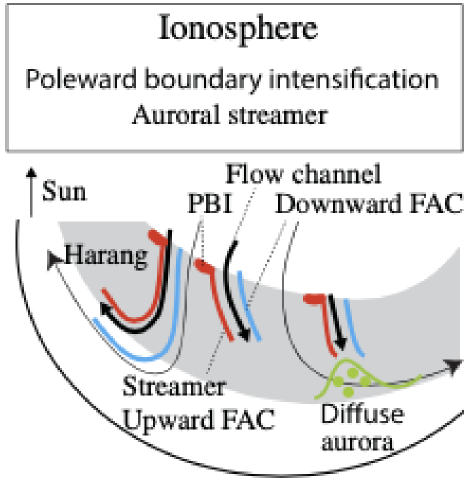

Nishimura et al., 2020

Large-scale structures are well characterized with statistical studies.

Models of Convection (E)

- Weimer Model:
  - DE driftmeter measurements binned for different solar wind and IMF conditions and geographical locations.
- Other models: Heppner-Maynard Model, Hardy Model, Heelis Model, AMGeO/AMIE

Models of Particle Precipitation (σ_P)

- Ovation Prime:
  - DMSP particle data binned for different solar wind and IMF conditions and geographical locations.
- Other models: Ovation SM, Fuller-Rowell Evans Model, Hardy Model, FTA Model

Weimer Model: Reproduces 2-cell convection pattern.

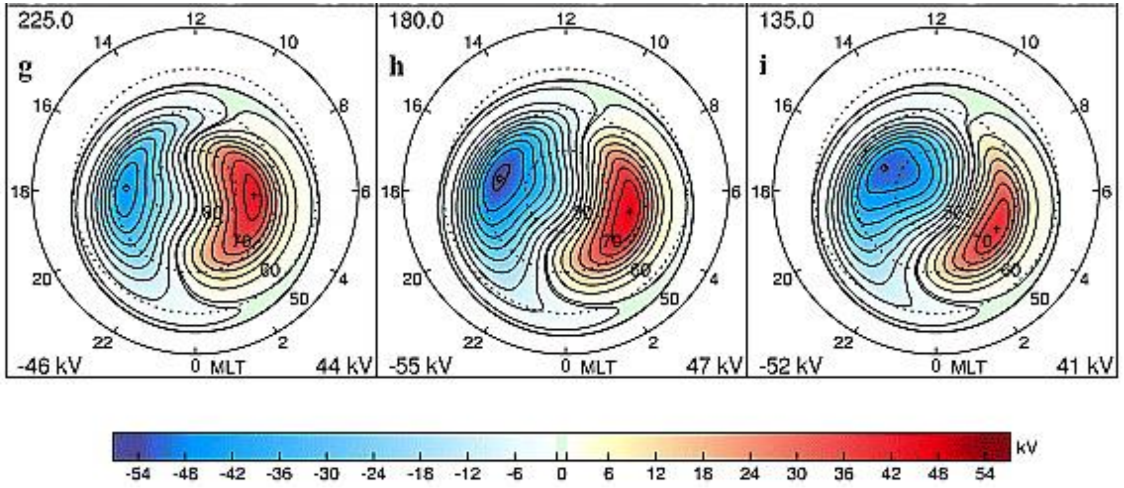

Weimer, 2005

Ovation Prime Model: Reproduces auroral oval.

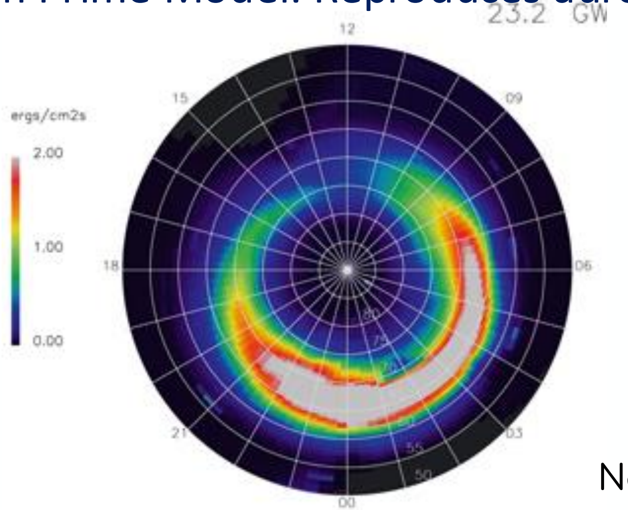

Newell et al., 2010

Comparison of large-scale model results with real data

Spatial, temporal and amplitude variations can not be captured with empirical models.

$$\boxed{Q_{JH}} = \sigma_P[\boldsymbol{E} + u_n \times \boldsymbol{B}]^2$$

Fuller-Rowel and Evans Model

Polar UVI

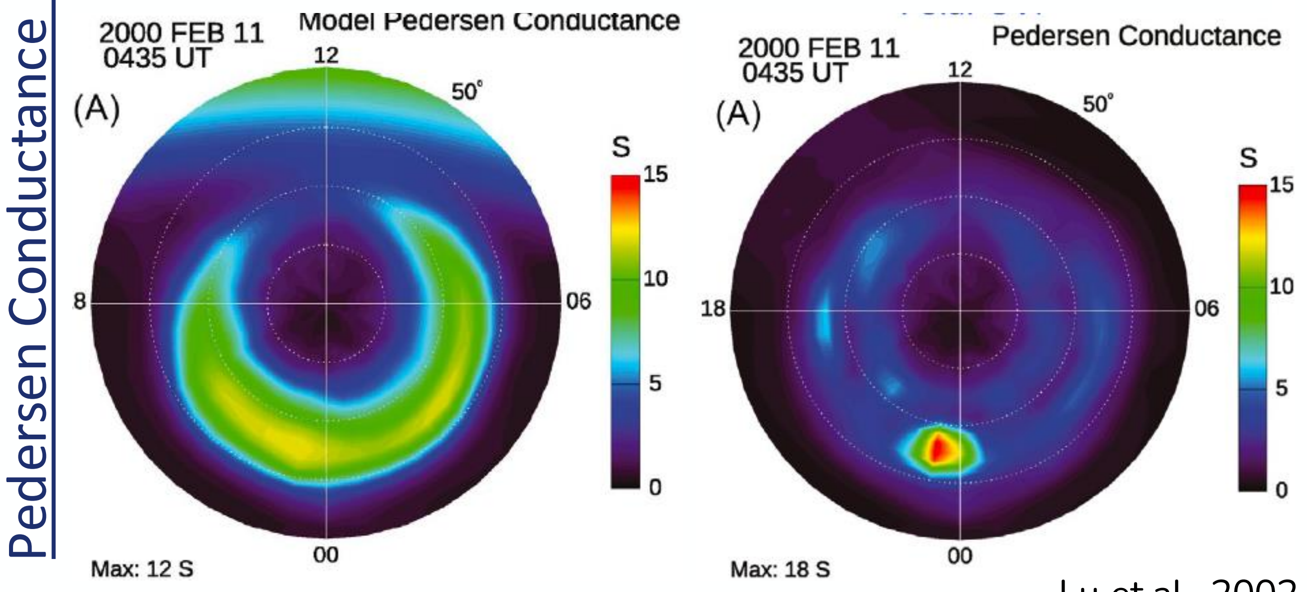

Lu et al., 2002

Derived from DE-2 ion driftmeter

Time shifted model estimates

Weimer 2005 Electric Potential Model

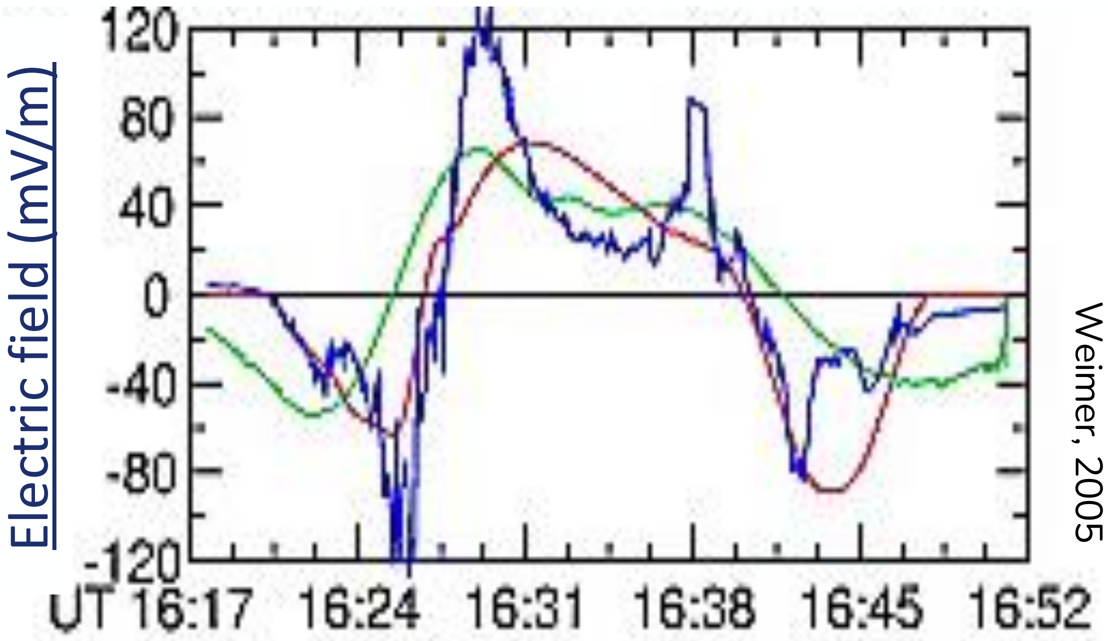

Weimer, 2005

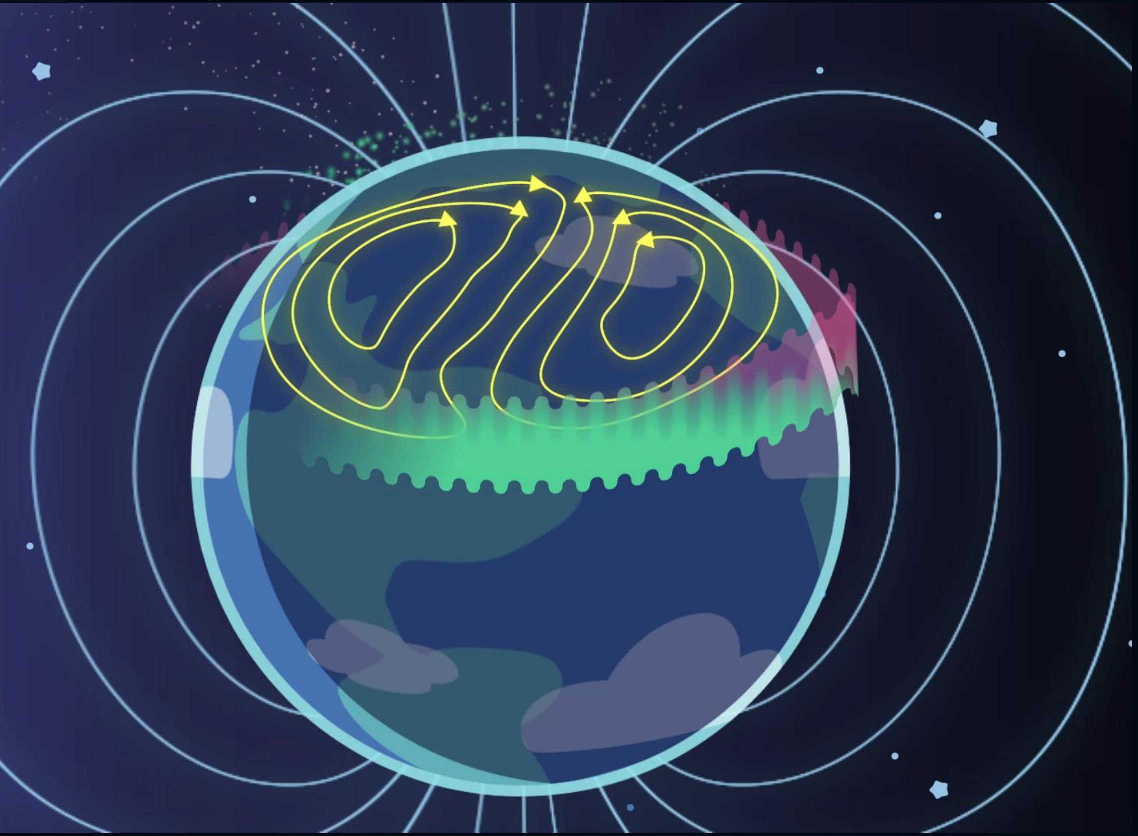

How can we utilize PFISR data to solve long-known problems in numerical models?

MHD model output characterizes the multi-scale variability of the magnetospheric drivers.

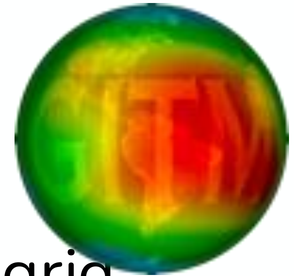

- Solves Navier-Stokes equations on 3D, altitude based non-uniform grid, assuming non-hydrostatic solution.
- Input: Solar wind plasma parameters, IMF vector measurements, F10.7
  - Convection electric field models: AMIE, Weimer, Heelis, RIM, AMGeO
  - Particle precipitation models: AMIE, OvationPrime, OvationSME, RIM, FRE, AMGeO, FTA
- Heating: EUV, Joule, auroral, conduction and chemical heating
- Cooling: NO, CO2 and O2 radiative cooling
- Species are:
  - Neutrals: O, O2, N(2D), N(2P), N(4S), N2, NO, H and He
  - Ions: O+(4S), O+(2D), O+(2P), O+2, N+, N+2, NO+, H+ and He+
- Output: Plasma and neutral density, temperature, ion and electron velocity, neutral winds

Ridley, Deng and Toth, JASTP, 2006

Meso-scale electric fields observed by PFISR

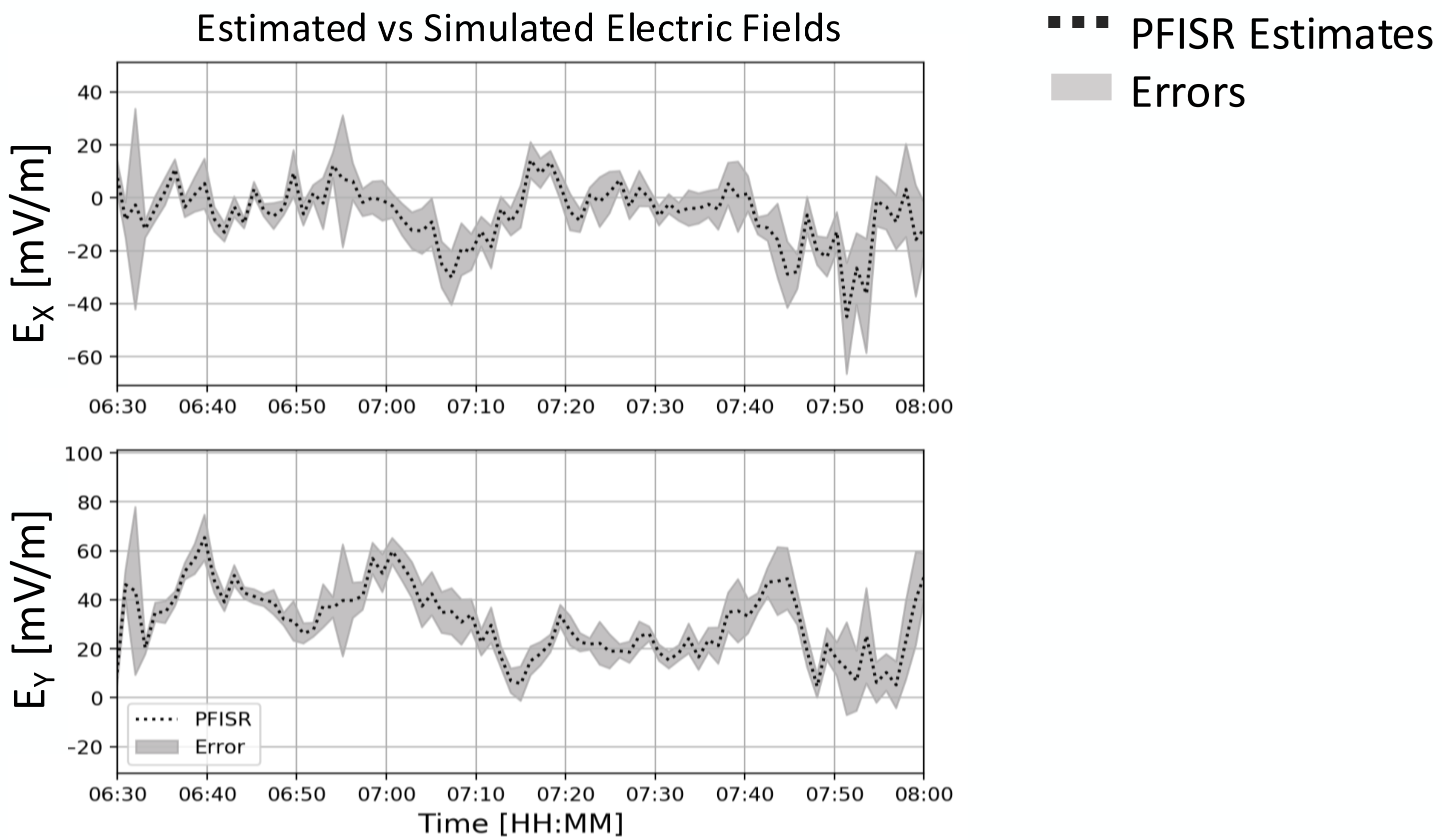

* Profiles extracted from upper boundary.

Comparison between PFISR E fields and Weimer-driven GITM Simulations

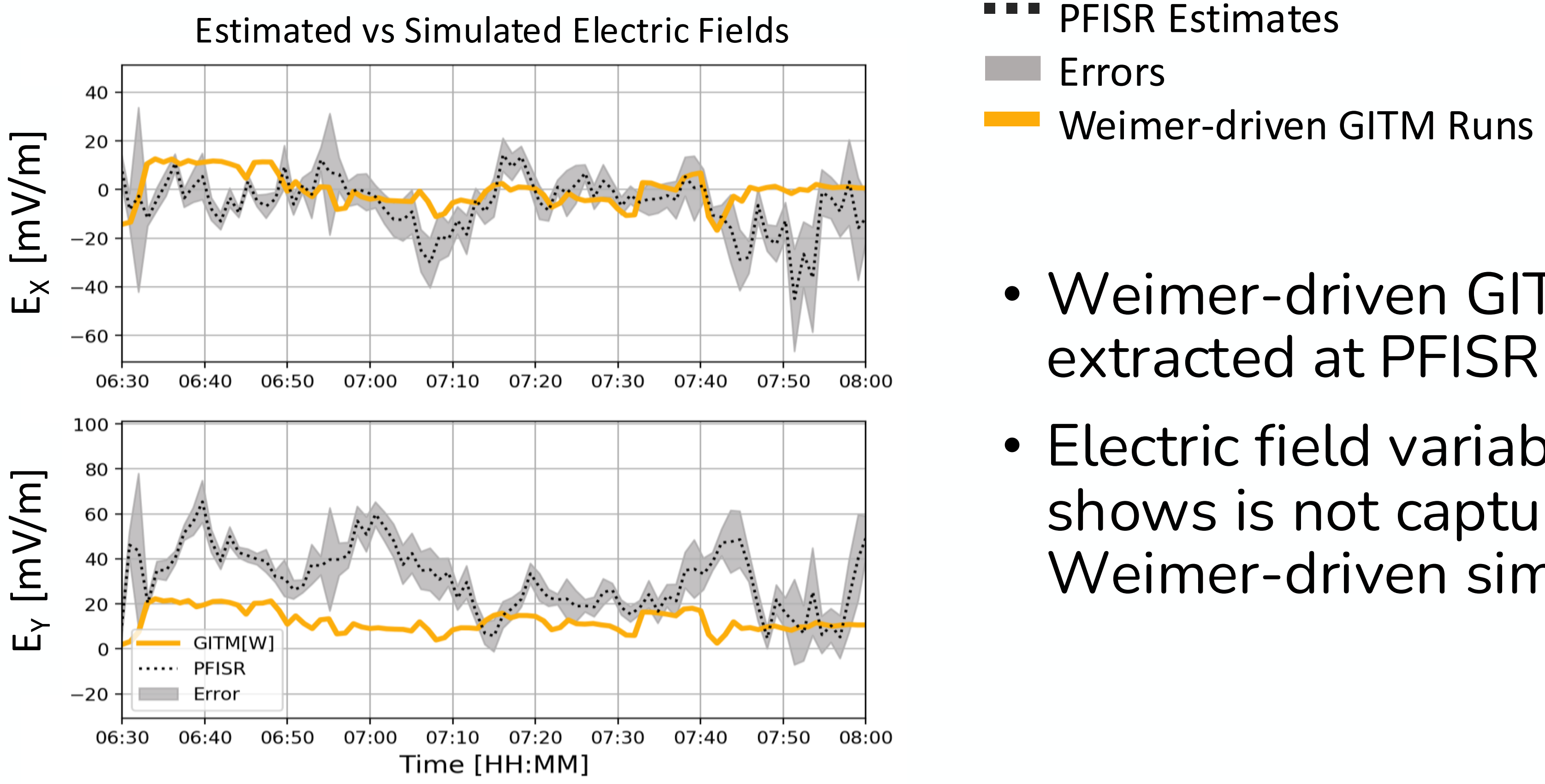

- Weimer-driven GITM results are extracted at PFISR location.
- Electric field variability that PFISR shows is not captured in the Weimer-driven simulation results.

* Profiles extracted from upper boundary.

ISR measurements can provide information on electric field and particle precipitation.

Beam Layout

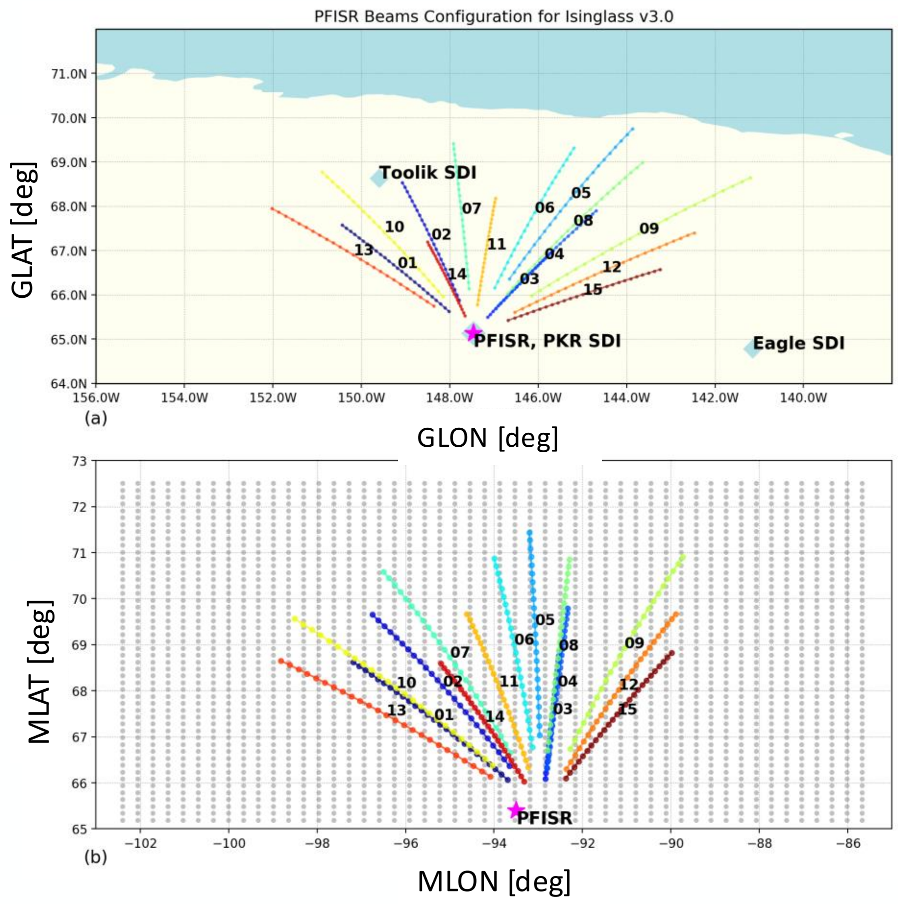

Modelling:

- PFISR aiding the ISINGLASS experiment with 15 beams operating [Lynch et al., Clayton et al., 2019a, b]
  - LOS velocity measurements to derive Electric fields on a 2D grid.
  - Temporal resolution [66 seconds]
  - Spatial resolution [0.05° in latitude and 0.3° in longitude, ~10 km]

Validation:

- PFISR plasma measurements along Beams
- Three SDI (Scanning Doppler Imagers) measurements for neutral wind

Meso-scale electric fields with the High-latitude Input for Meso-scale Electrodynamics (HIME) Framework

Using down-sampled PFISR 2D electric field estimates, potential differences can be merged with a global empirical potential model to drive global I-T models and investigate the role of meso-scale electric fields.

Electric Field Estimates:

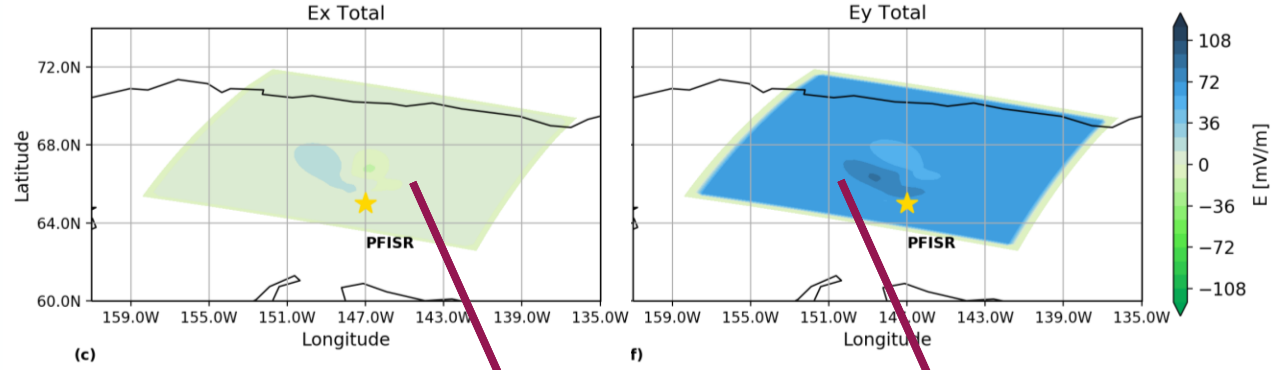

Conversion:

$$\Delta\phi_x = -\int_{x_1}^{x_2} E_x \, dx \qquad \Delta\phi_y = -\int_{y_1}^{y_2} E_y \, dy$$

Merging:

Default Input

HIME

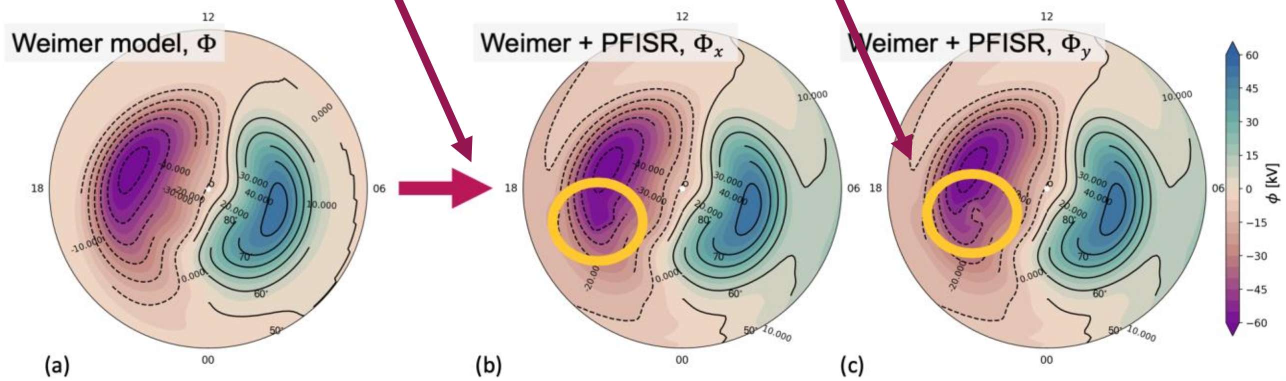

Ozturk et al., 2020

Meso-scale Electric Fields in HIME-driven GITM Simulations

Electric Fields:

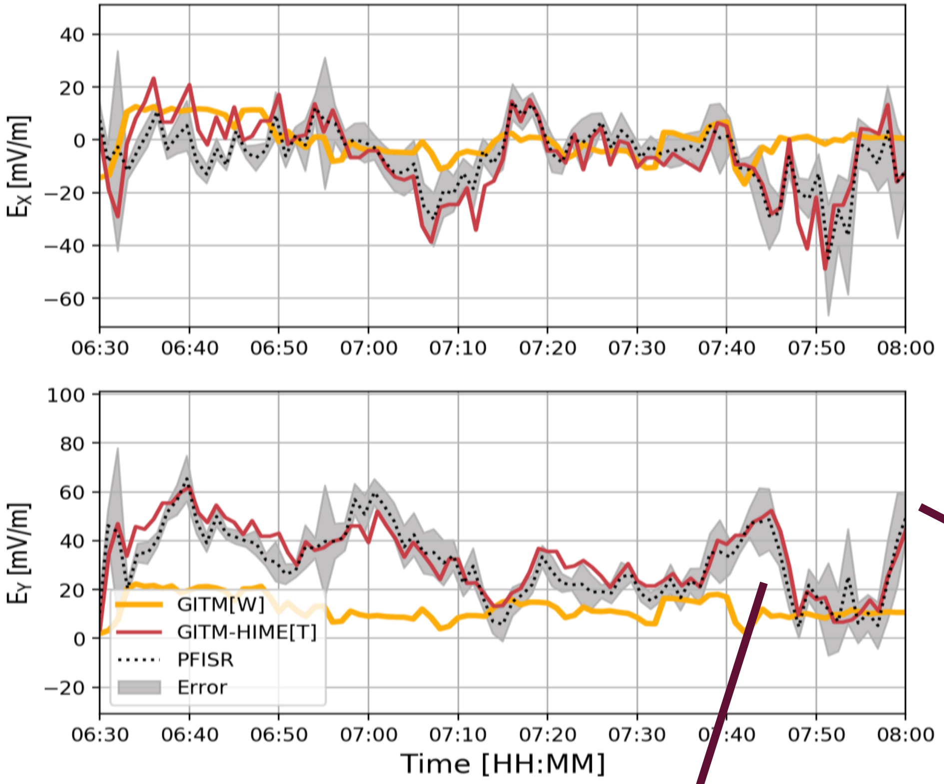

* Profiles extracted from upper boundary.

Both variability and amplitude are better captured with HIME.

- PFISR Estimates
- Errors
- Weimer-driven GITM Runs
- HIME-driven GITM Runs

The locally deposited energy increases in HIME-driven simulation compared to Weimer-driven simulation.

Joule Heating:

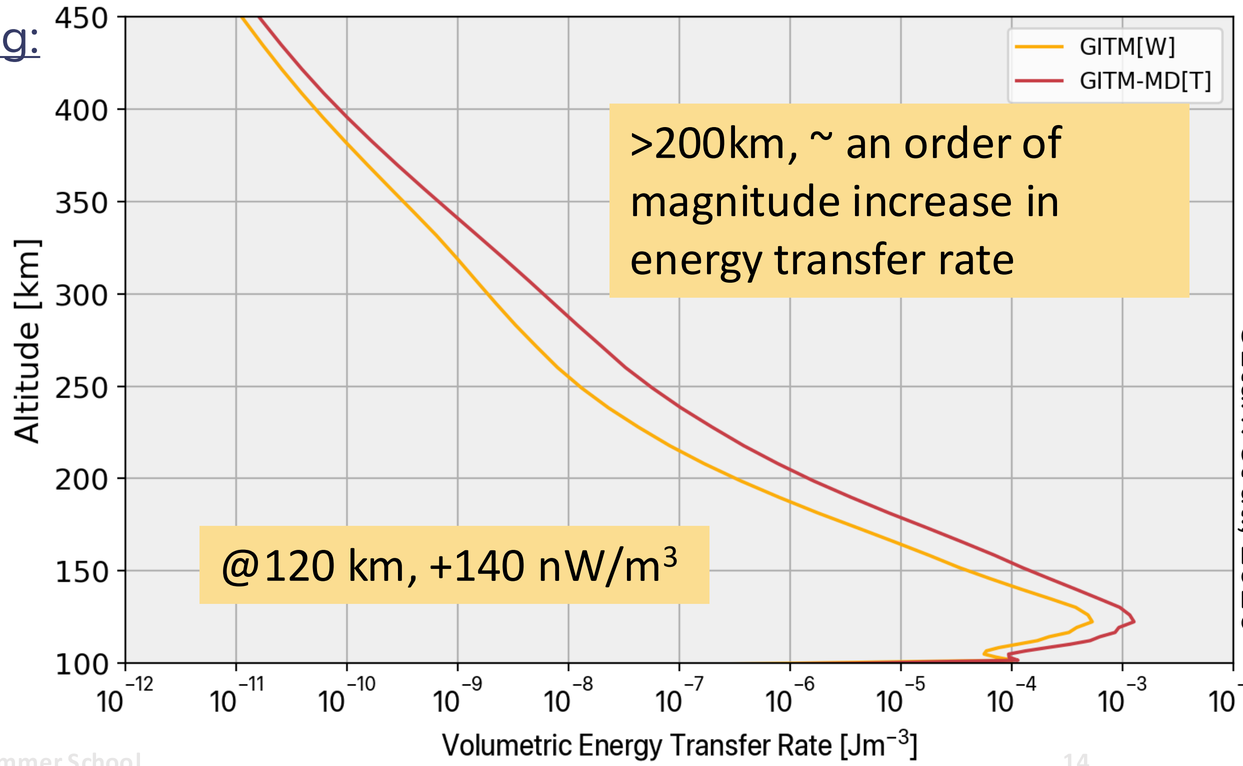

Ozturk et al., 2020

Modeled ion and electron temperature response

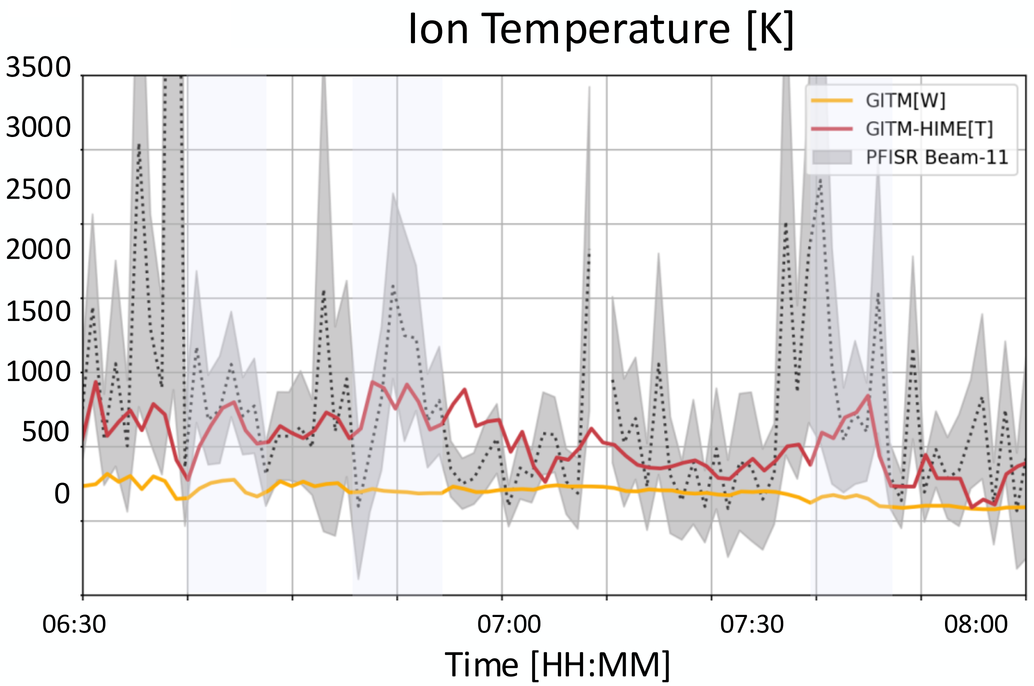

* Profiles extracted from 245 km.

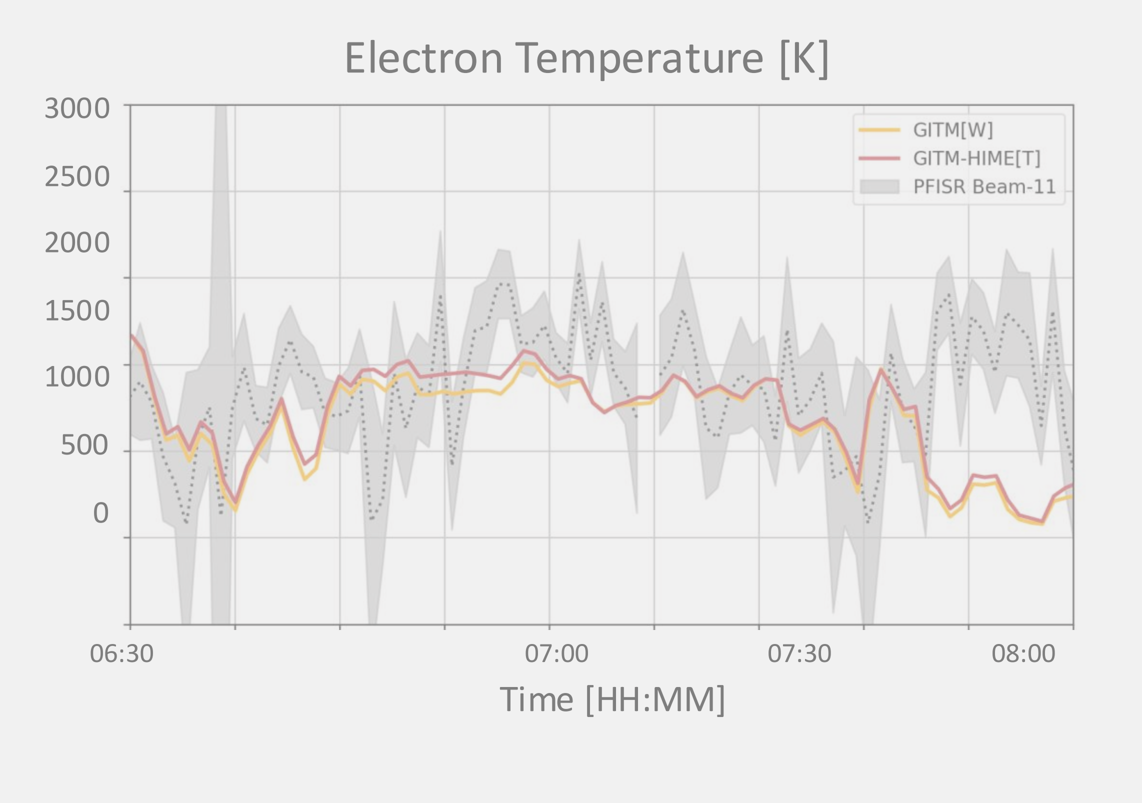

Modeled ion temperature captures variability better with enhancements up to 700 K when HIME is used.

Modeled ion and electron temperature response

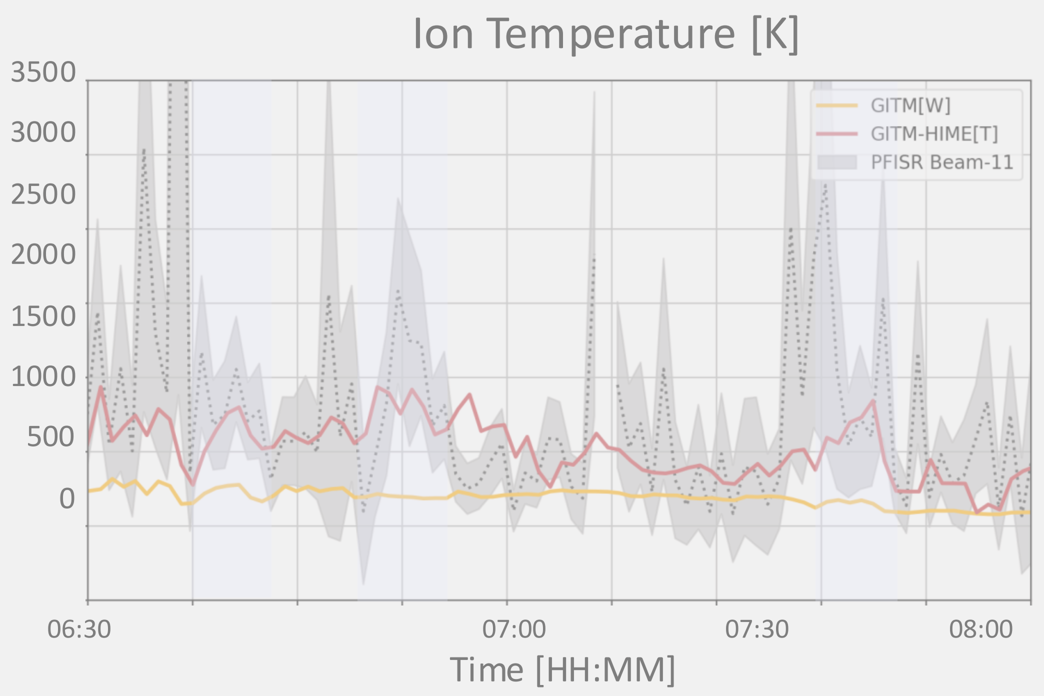

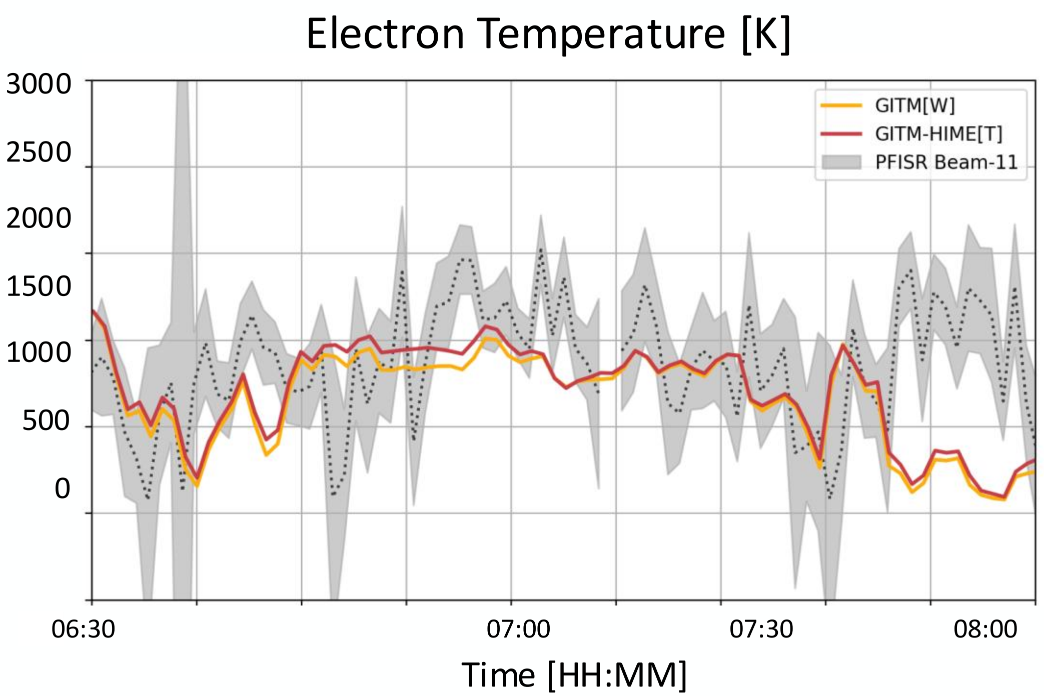

* Profiles extracted from 245 km.

Modeled electron temperature is not as responsive to meso-scale driving as ions.

Insights from the modelled electron density response

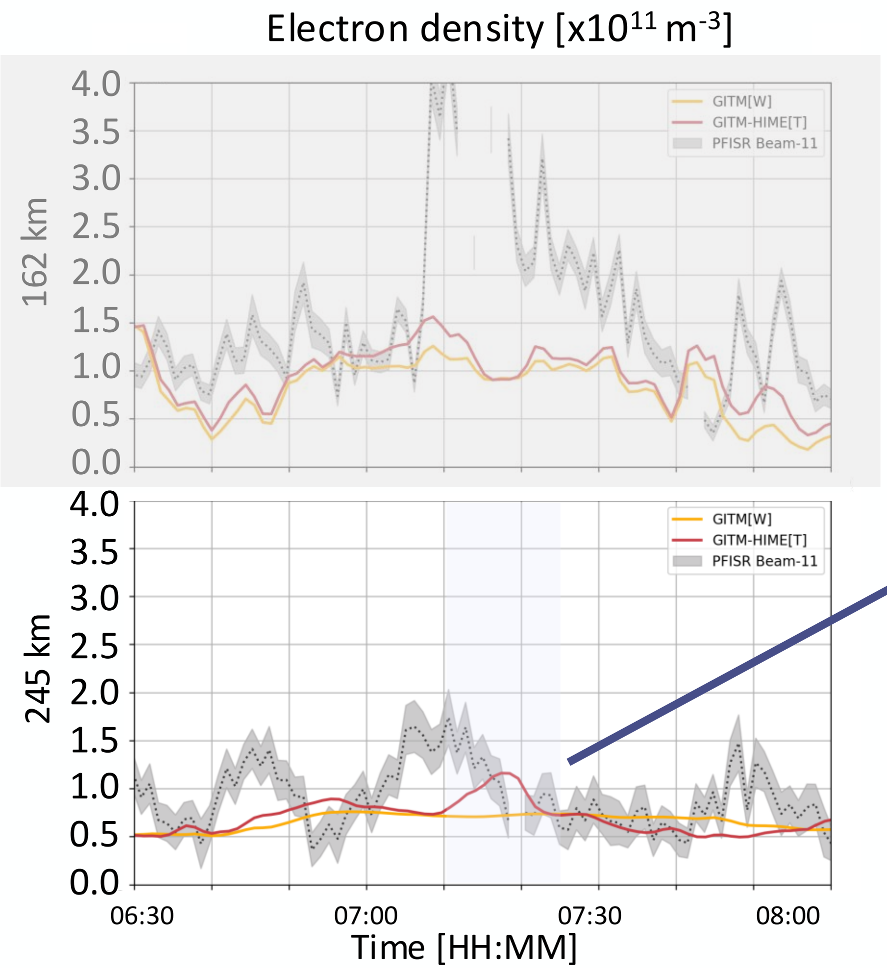

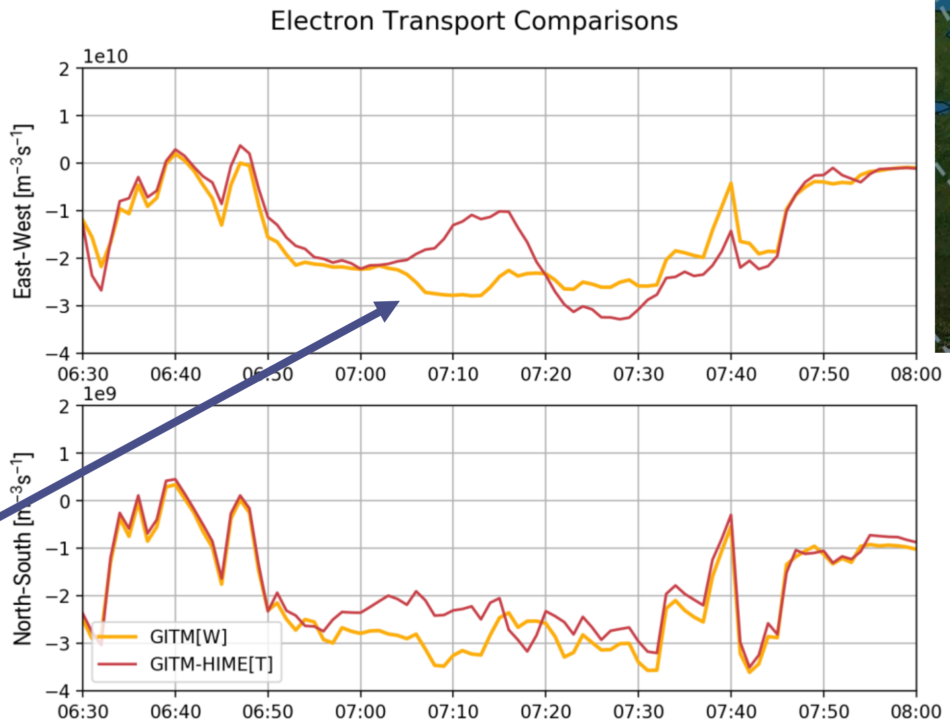

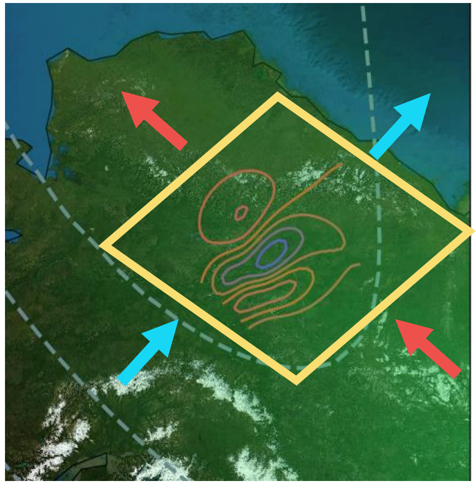

~ Up to %100 increase in simulated electron density likely due decreased westward transport mechanism.

Insights from the modelled electron density response

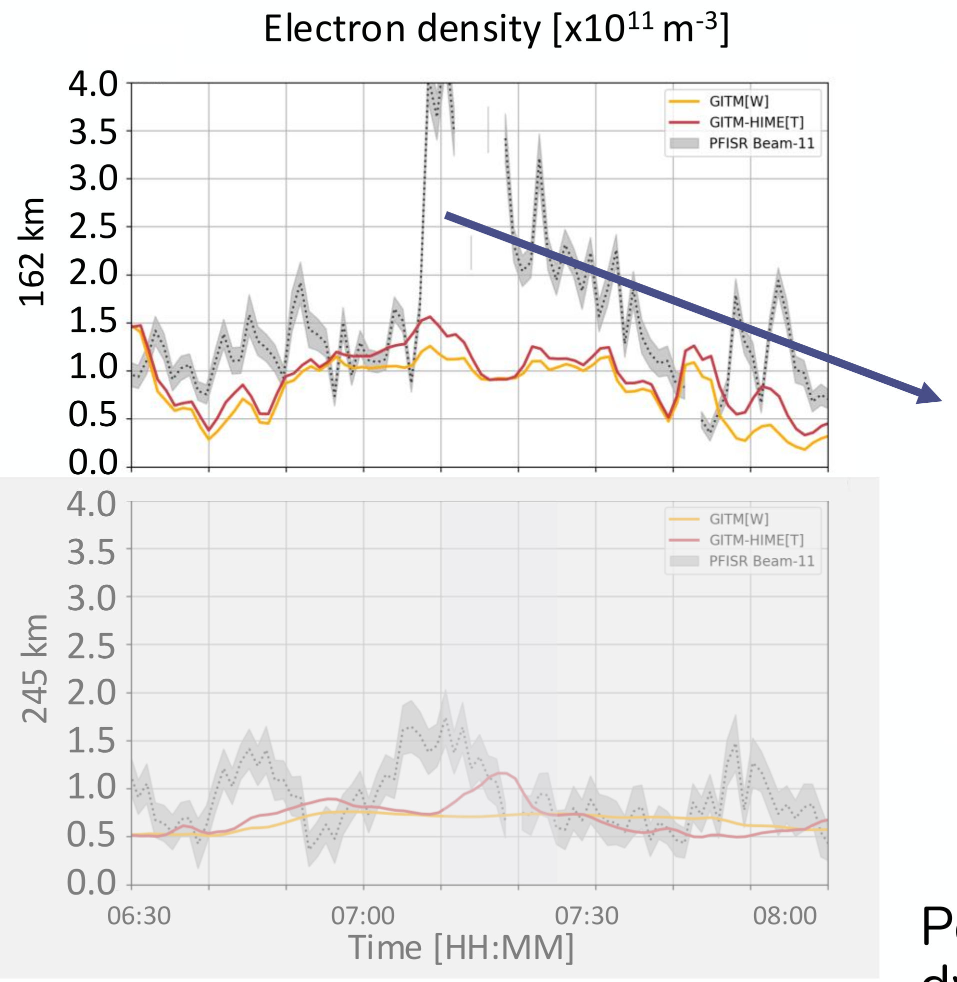

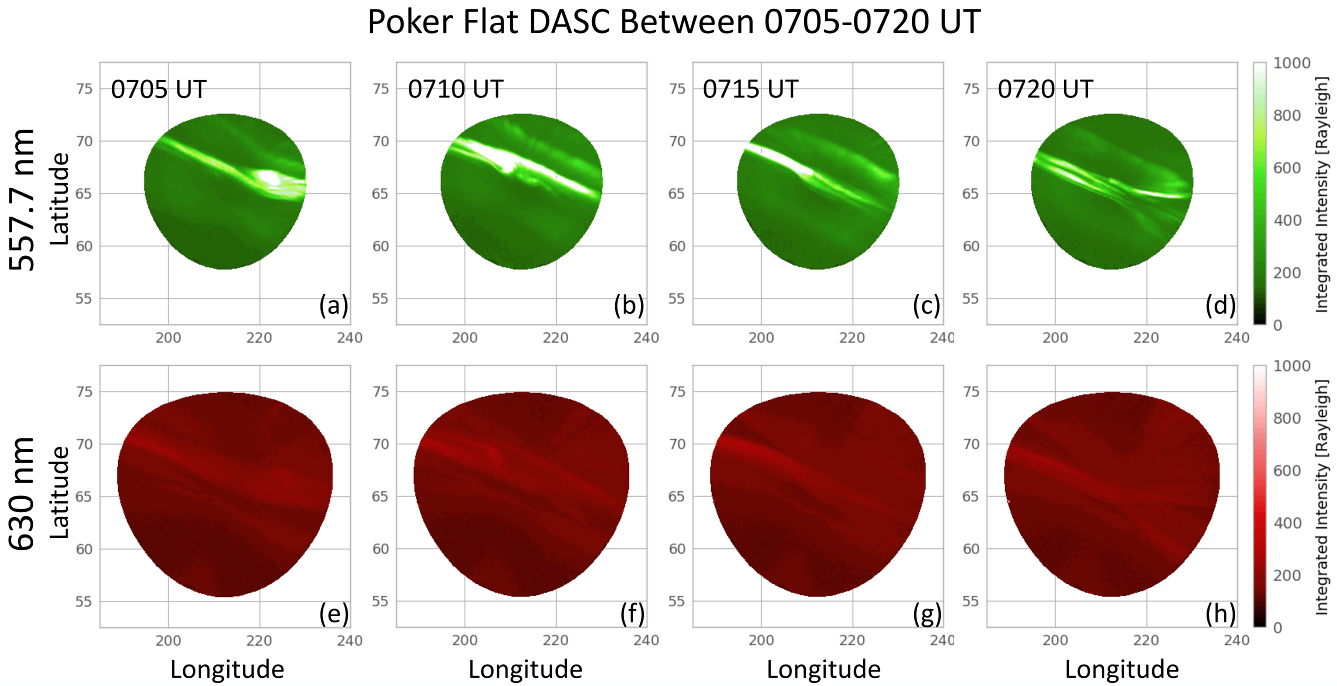

Poker Flat DASC, co-located with PFISR, shows bright dynamic aurora over the same region.

New techniques to help understand meso-scale structures

- New machine learning techniques based on representation learning (SimCLR).
- A two-stage learning algorithm applied to Poker FLAT DASC images show various different classes.
- PFISR can help provide further precipitation characteristics to achieve a complete picture of the electrodynamic properties of meso-scale phenomena.

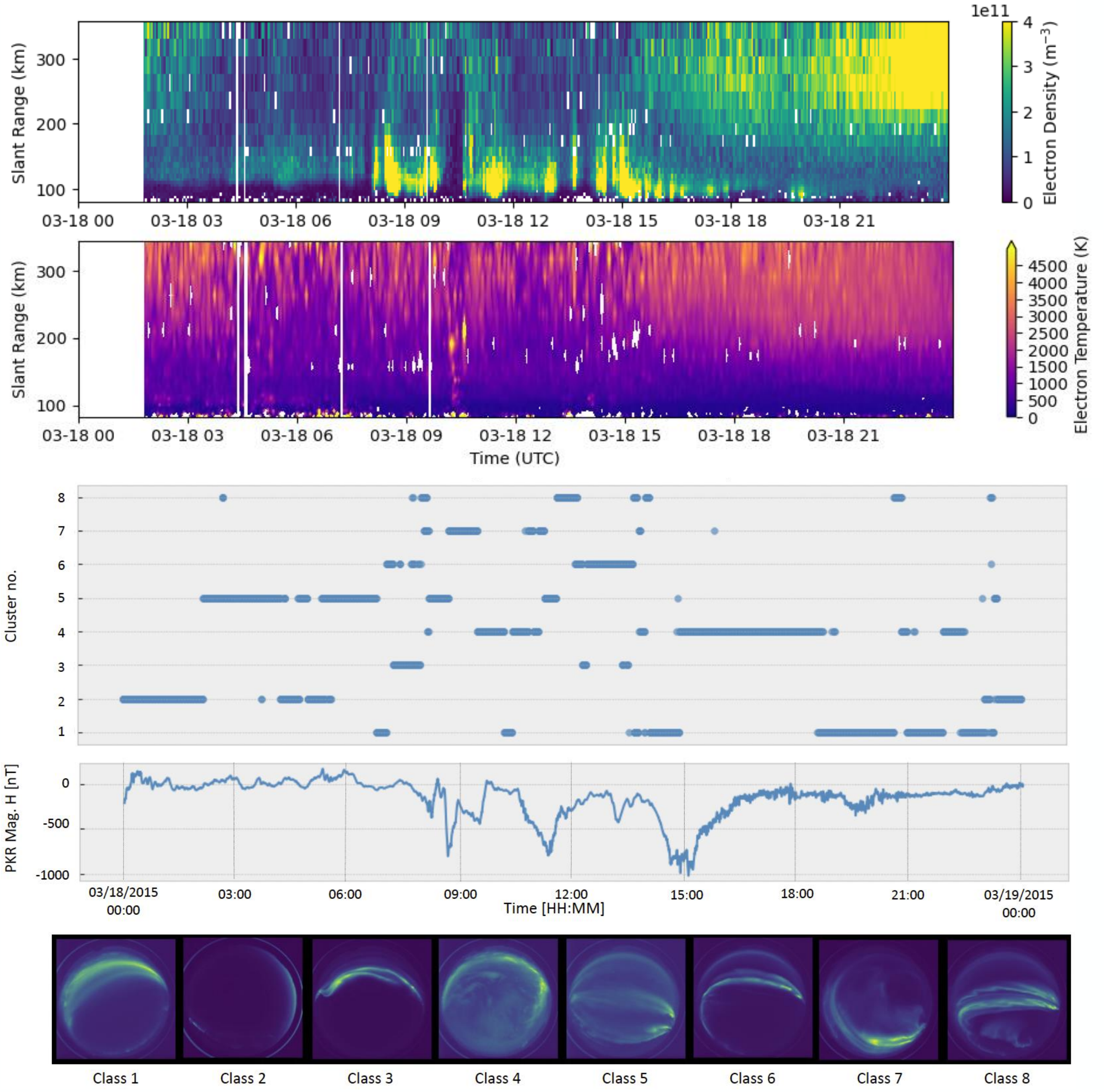

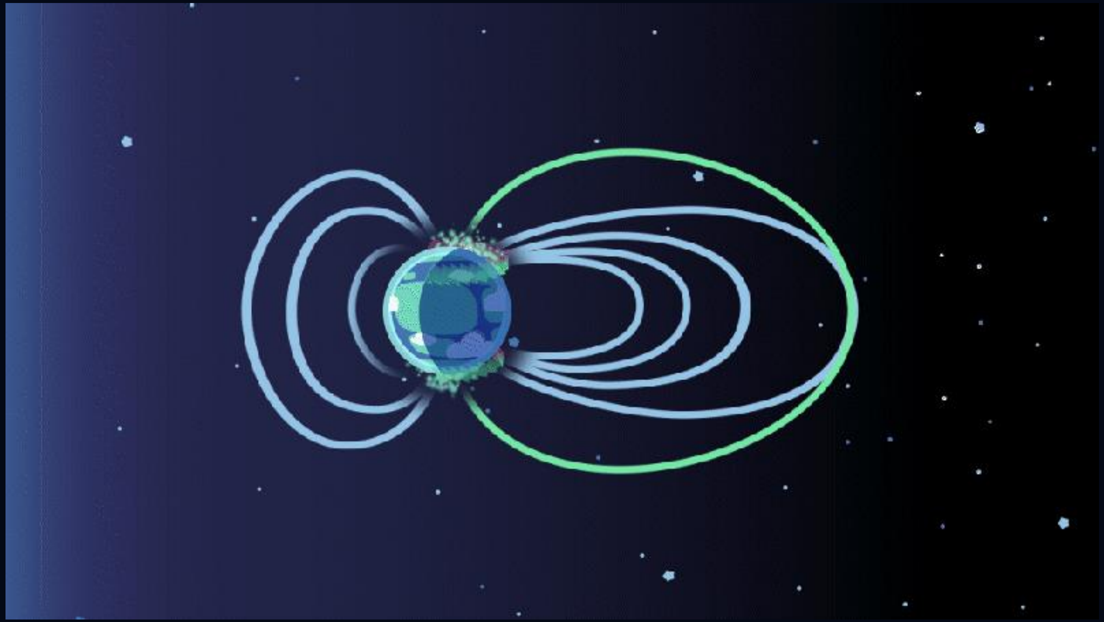

How can we utilize the PFISR data to gain better insight on coupled processes across the M-I-T system?

PFISR is unique in its ability to contextualize different geospace events

- Poker Flat Incoherent Scatter Radar (PFISR) measurements show a strong depletion of electron density.
- Ion perturbations less than 10 minutes.
- Poker Flat magnetometer signature shows a sharp drop.

A tell-tale sign of SSC.

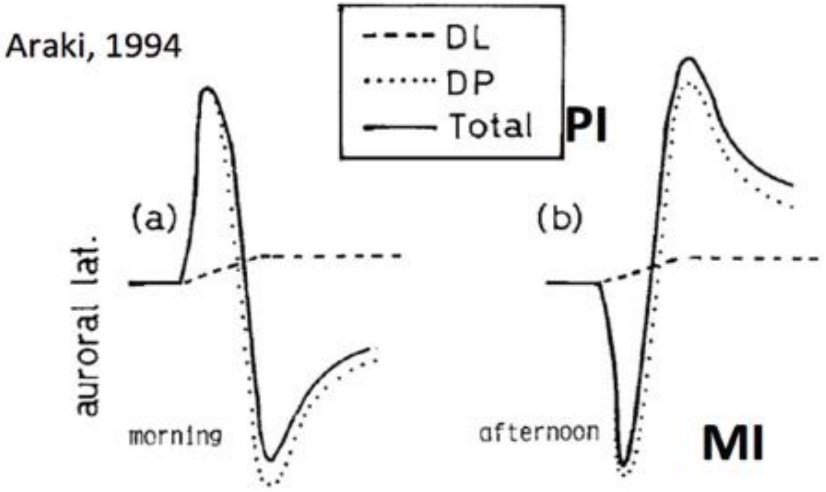

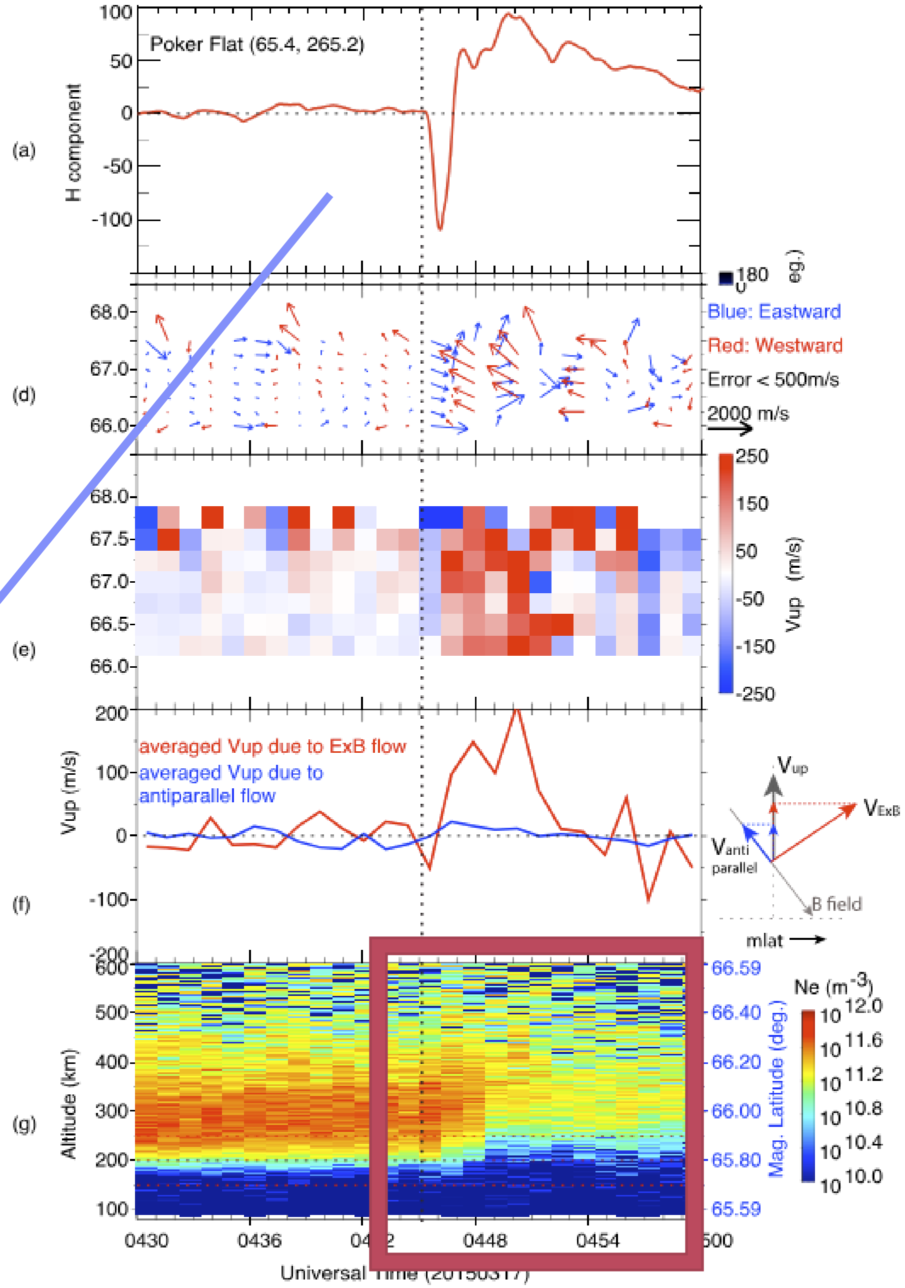

Solar wind and IMF values during the 2015 St. Patrick's Day Storm

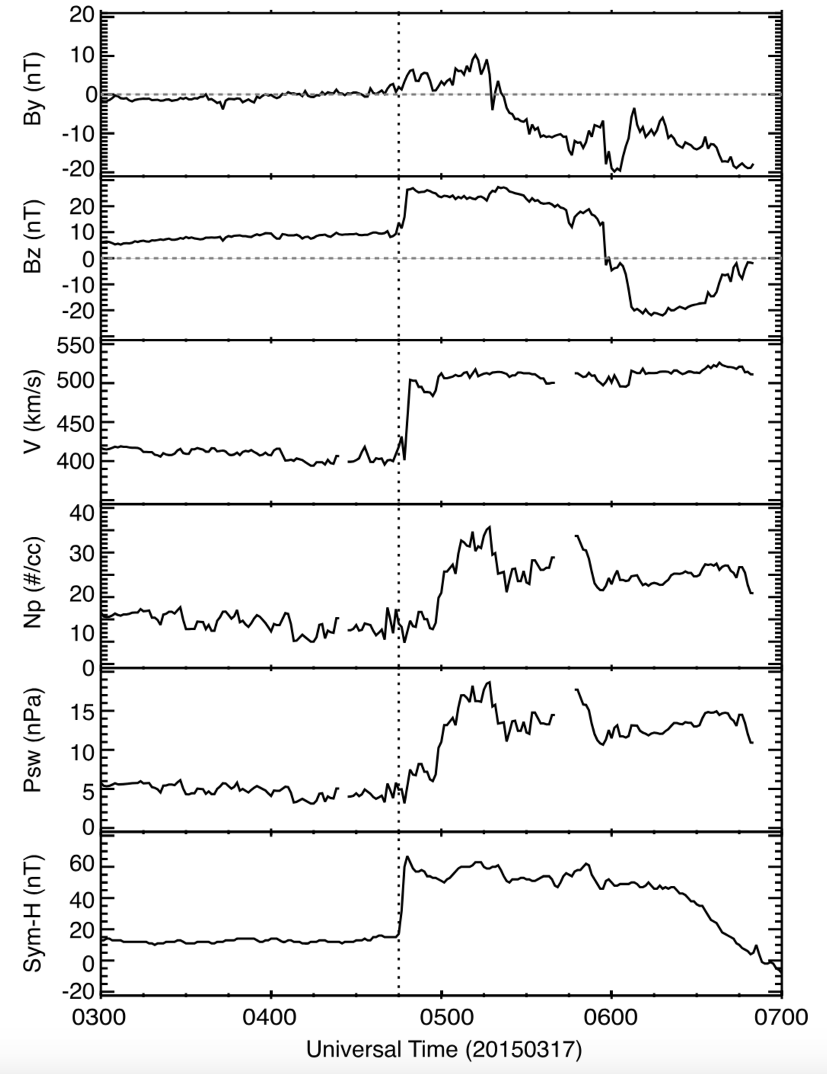

- Kp 8, min Sym-H -234 nT.
- Caused by an ICME.

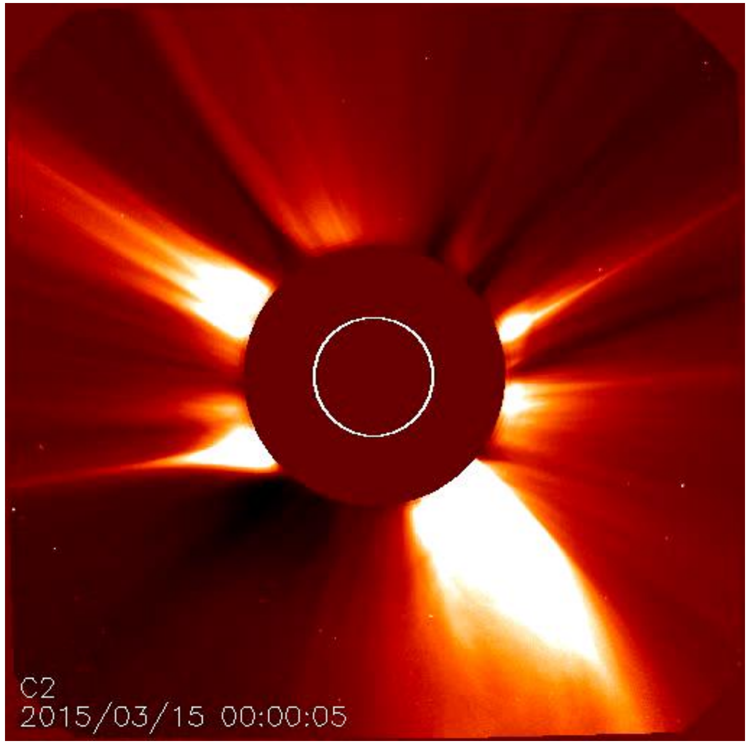

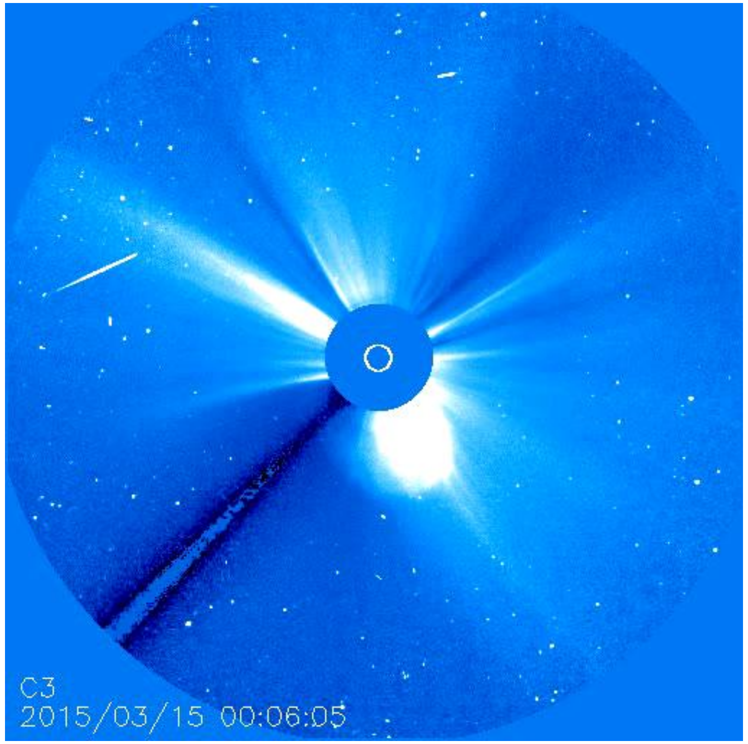

Perturbations by drivers could be investigated within the MHD domain.

- GM: Block Adaptive Tree Solarwind Roe Upwind Scheme (BATS-R-US) *[Powell et al., 1999; Toth et al., 2005]*
- IM: Comprehensive Inner Magnetosphere-Ionosphere Model *[Fok., et al., 2014; 2021]*
- IE: Ridley Ionosphere Model (RIM) *[Ridley, et al., 2004]*
- Ideal MHD
- Domain size (GSM coordinates) – Geospace Configuration
    - X : 32 to -224 Re
    - Y, Z : -128 to 128 Re
- Virtual ground magnetometer grid 2°x2° up to 80° magnetic latitude, 1 min. output

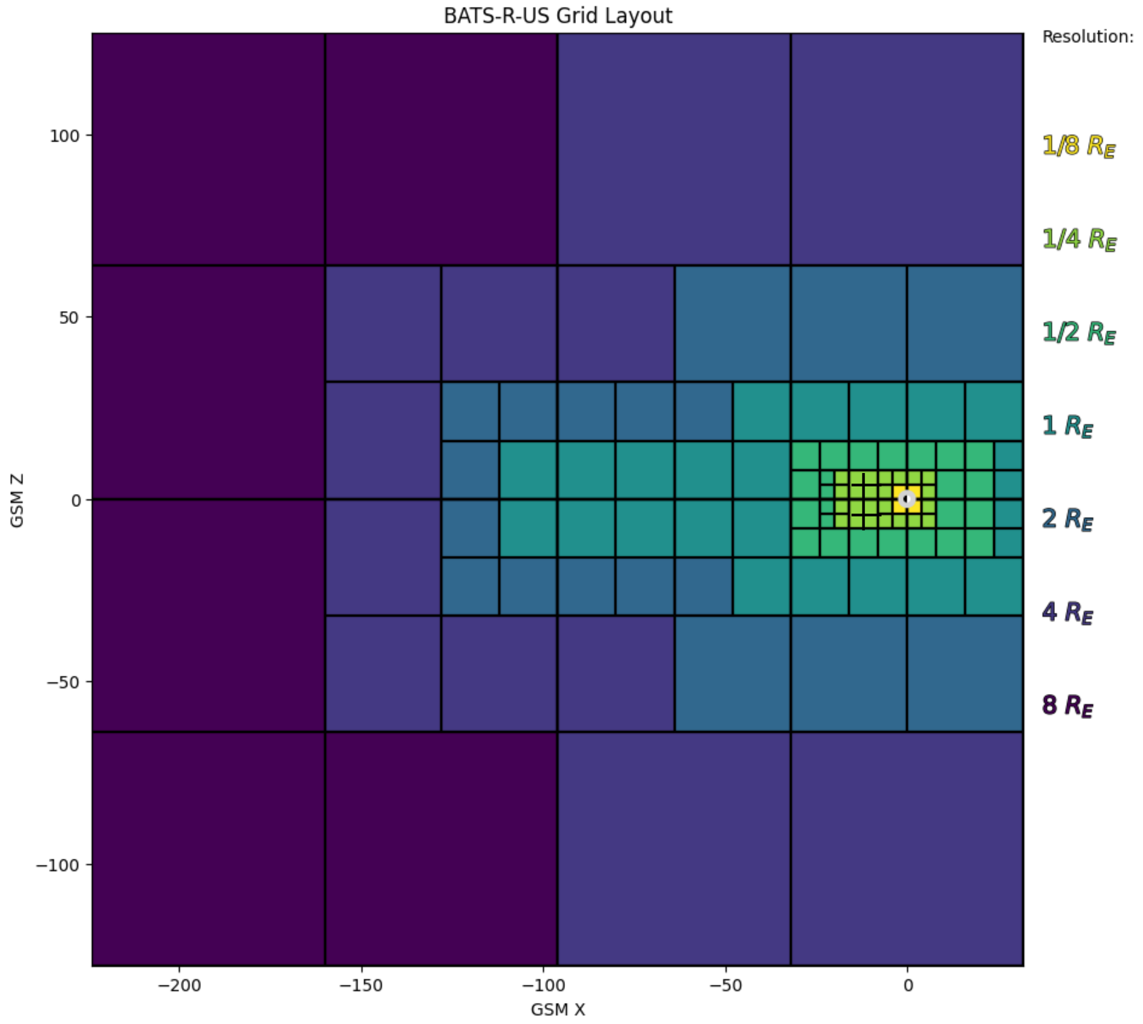

The ground magnetic perturbations as a response to the SSC

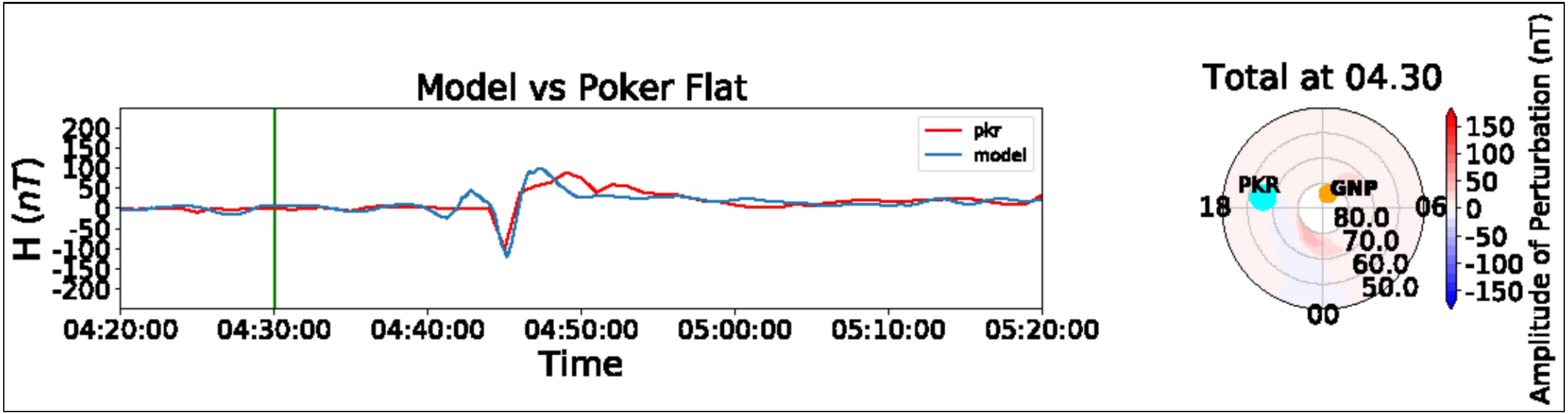

- Model and Observation show good agreement at PKR* location, indicating that the MHD model well captures the ionospheric electrodynamics.
- Using Poker Flat magnetometer location to trace ionospheric and magnetospheric drivers of the perturbation.

Transient FACs and magnetospheric vortices are responsible for the perturbation.

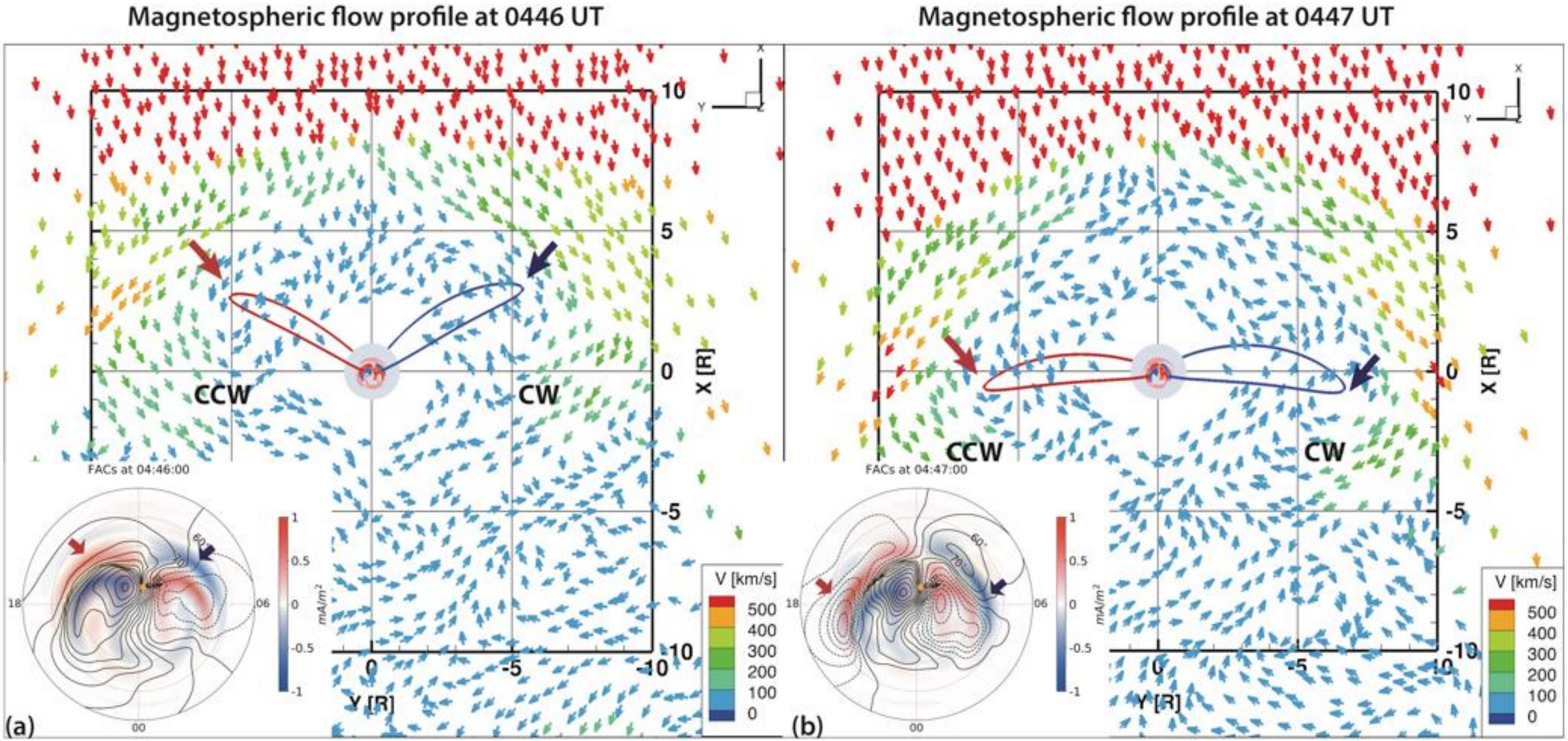

Ozturk et al., 2018

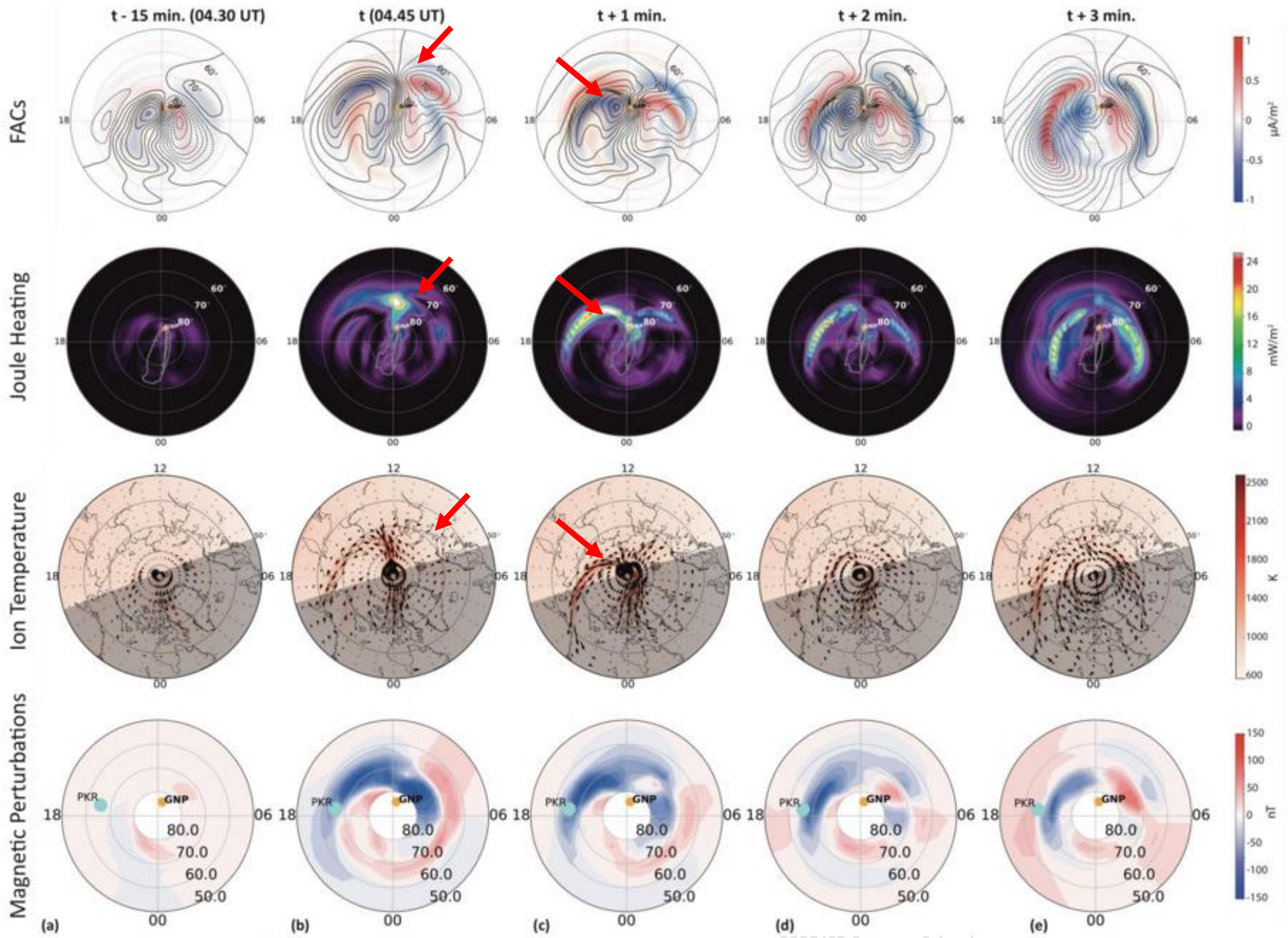

I-T Response

- Transient FACs in response to magnetospheric flows.
- Enhanced Joule Heating, varying in location with transient FACs.
- Short-lived ionospheric travelling convection vortices and enhanced ion temperatures.
- Global magnetic field perturbations in response to ionospheric currents.

The variations in the vertical ion and neutral temperature profiles during the event.

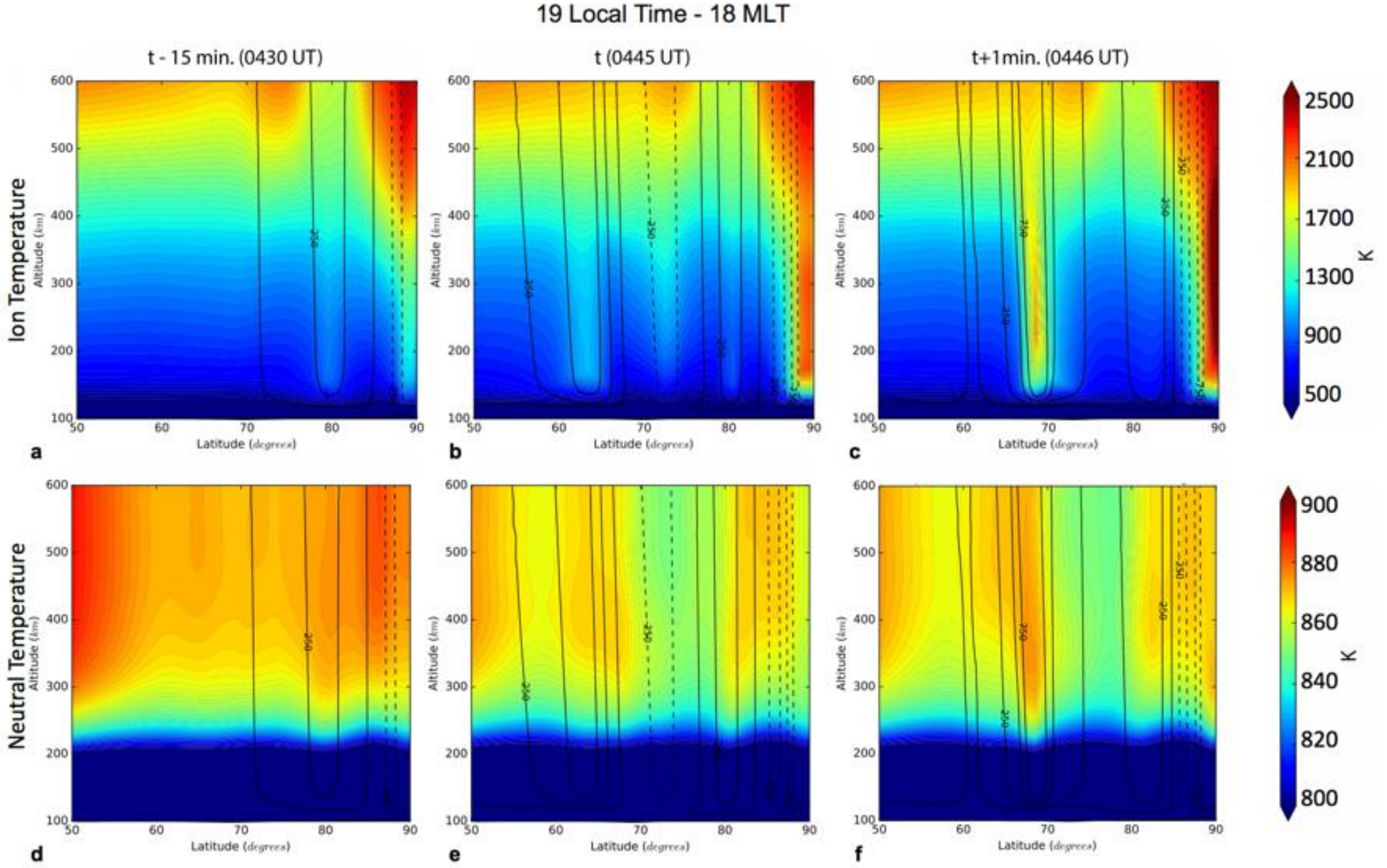

- **Ion convection profile is perturbed** during PI and MI phases
- **Ion temperature** is enhanced where the **convection flow** is higher
- Above **1000 K enhancement** in ion temperature
- ~**20 K enhancement** in neutral temperature during PI and MI phases

Ozturk et al., 2018

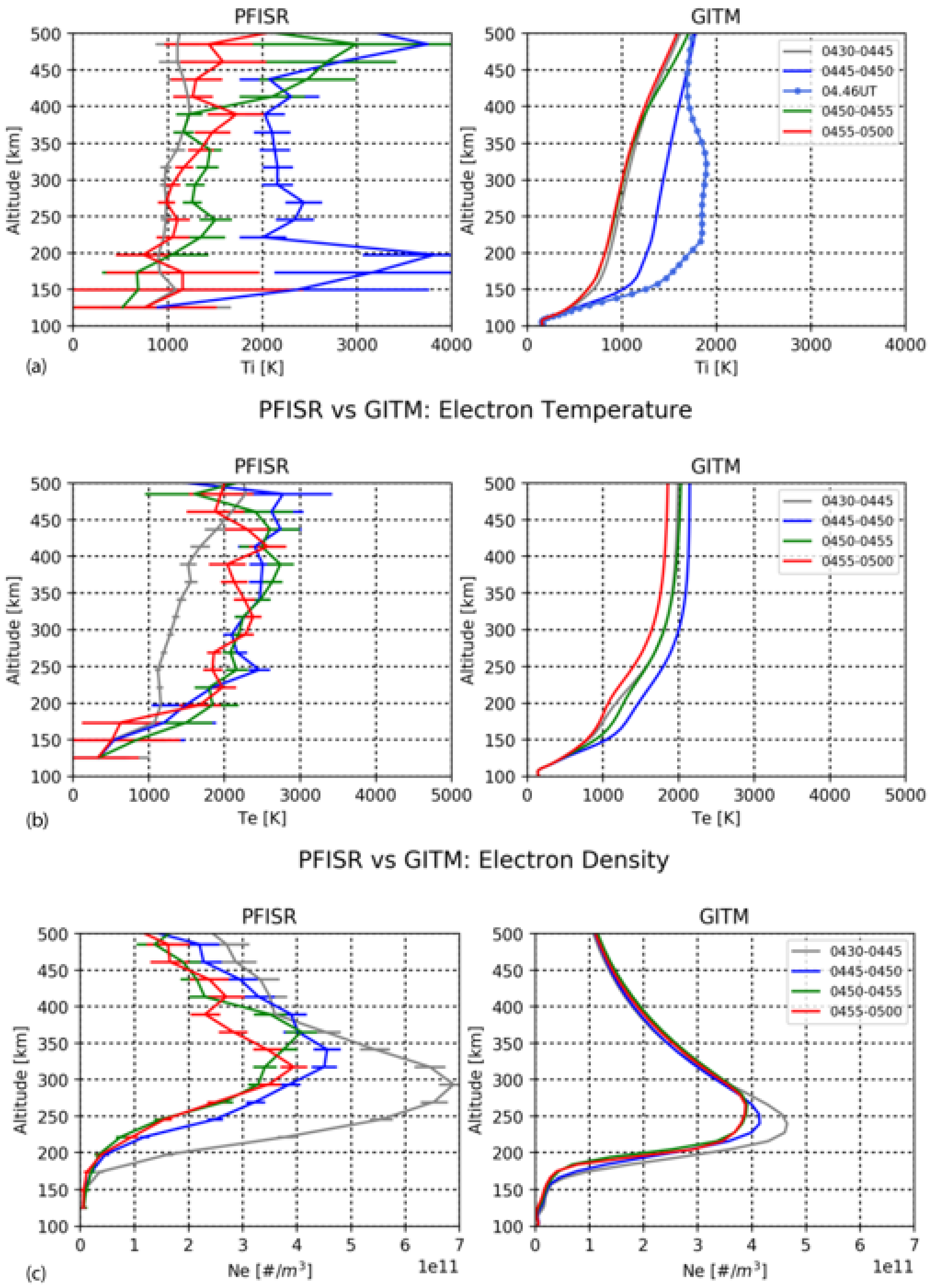

SSC related perturbations effect ions and electrons differently.

- 5-minute averaging of PFISR data to decrease SNR
- **Ion temperature enhancement** peak at 200 km
  - ~3500 K in PFISR
  - ~2000 K in GITM
- **Electron temperature enhancement**
  - ~1000 K in PFISR, stays high
  - ~500 K in GITM, drops below unperturbed state
- **Electron density peak** at
  - ~290 km in PFISR
  - ~240 km in GITM
- **Electron density drop**
  - ~%35 in PFISR
  - ~%15 in GITM

Zou et al., 2017; Ozturk et al., 2018

Various models exist or being developed to characterize ionospheric electrodynamics.

- For GITM alone, there exists a variety of model combinations that can specify precipitation and convection.
- These models can be:
  - Physics based (SWMF, GAMERA/MAGE, OpenGGCM, Vlasiator, etc.)
  - Empirical (FRE, Weimer, FTA, etc.)
  - Assimillative (AMGeO, AMIE, HIME etc.)

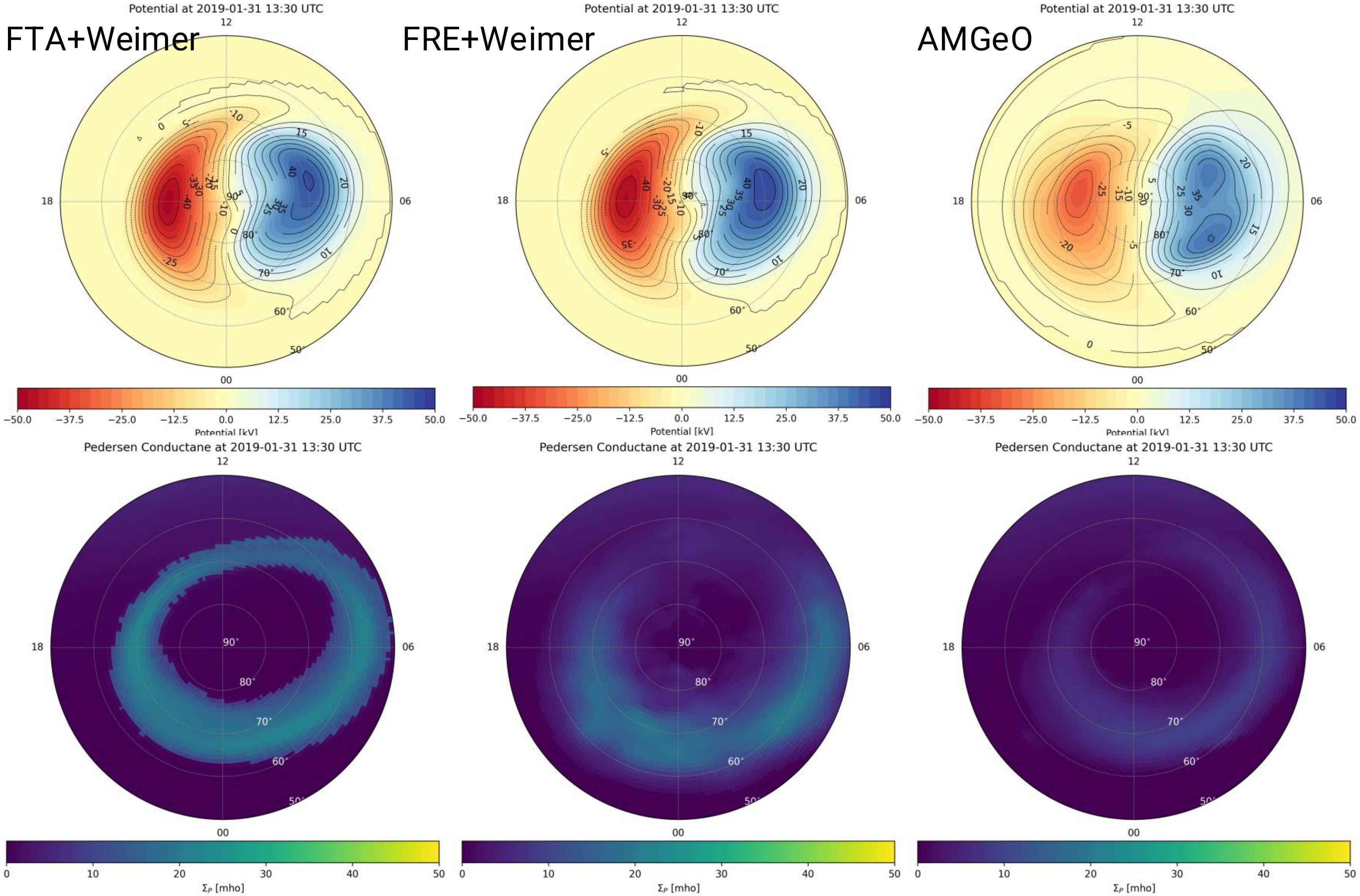

Validating the new models require self-consistent ground truth.

- FTA Model: Feature Tracking Model (Wu et al., 2021)
  - Polar UVI parameterized for AE and SME
- FRE: Fuller-Rowel and Evans Model (1987)
  - TIROS-NOAA statistical aurora maps parameterized for HPI
- AMGeO: Assimilative Mapping of Geospace Observations
  - SuperDARN and SuperMAG data products

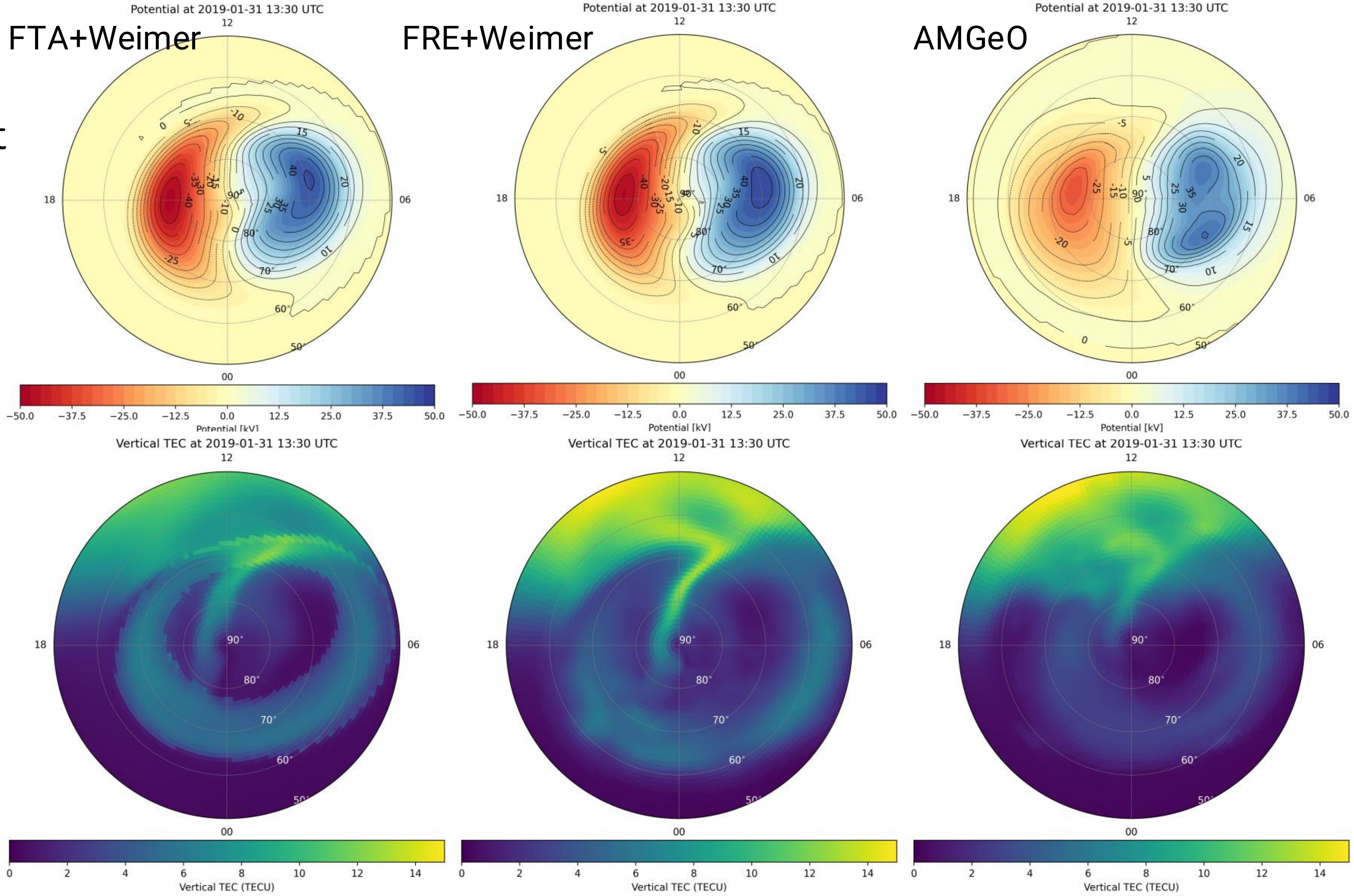

Validating the new models require self-consistent ground truth.

- Electron density is best captures with FRE model. (Lower energy electrons)
- Significant differences between all plasma parameters.

FTA+Weimer **FRE+Weimer** **AMGeO**

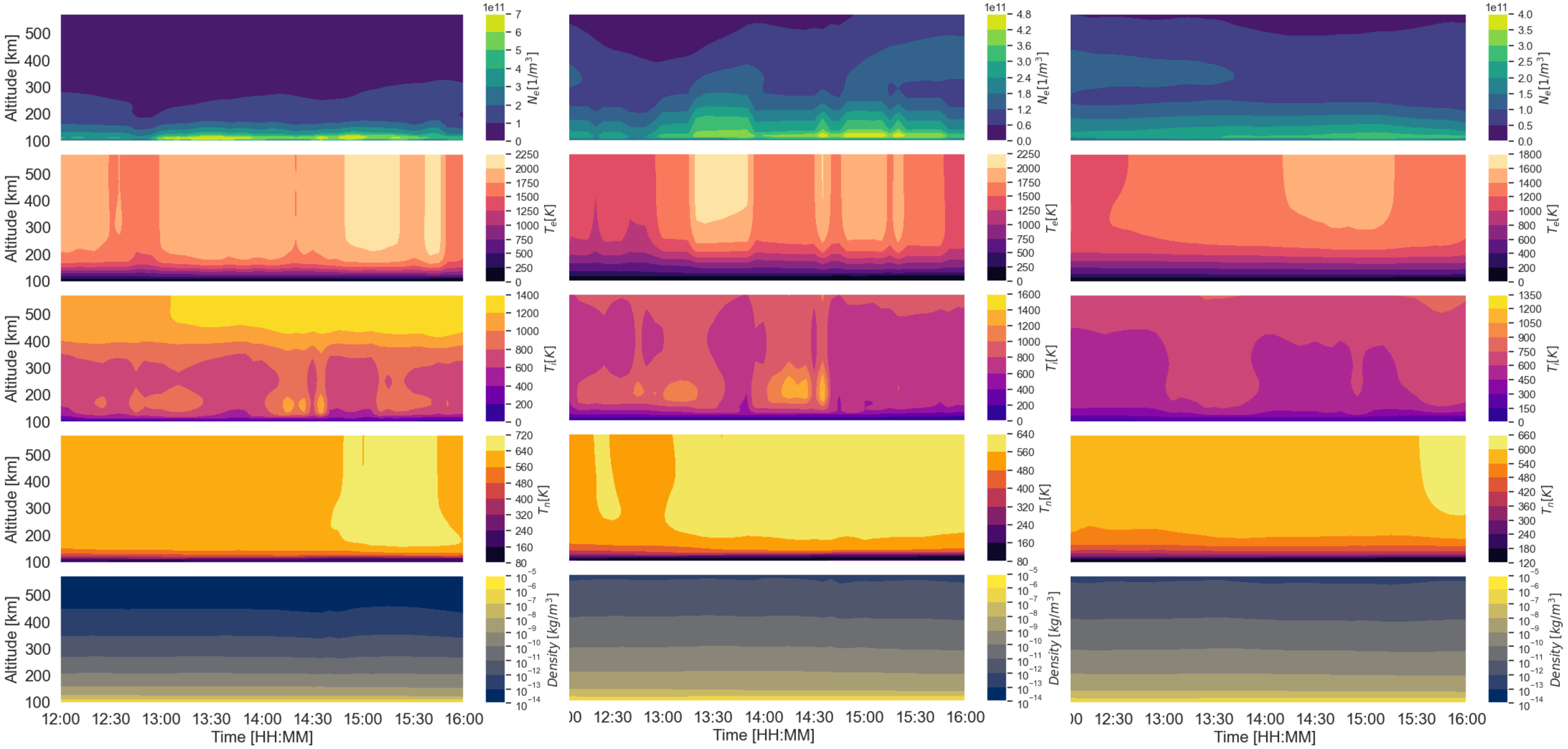

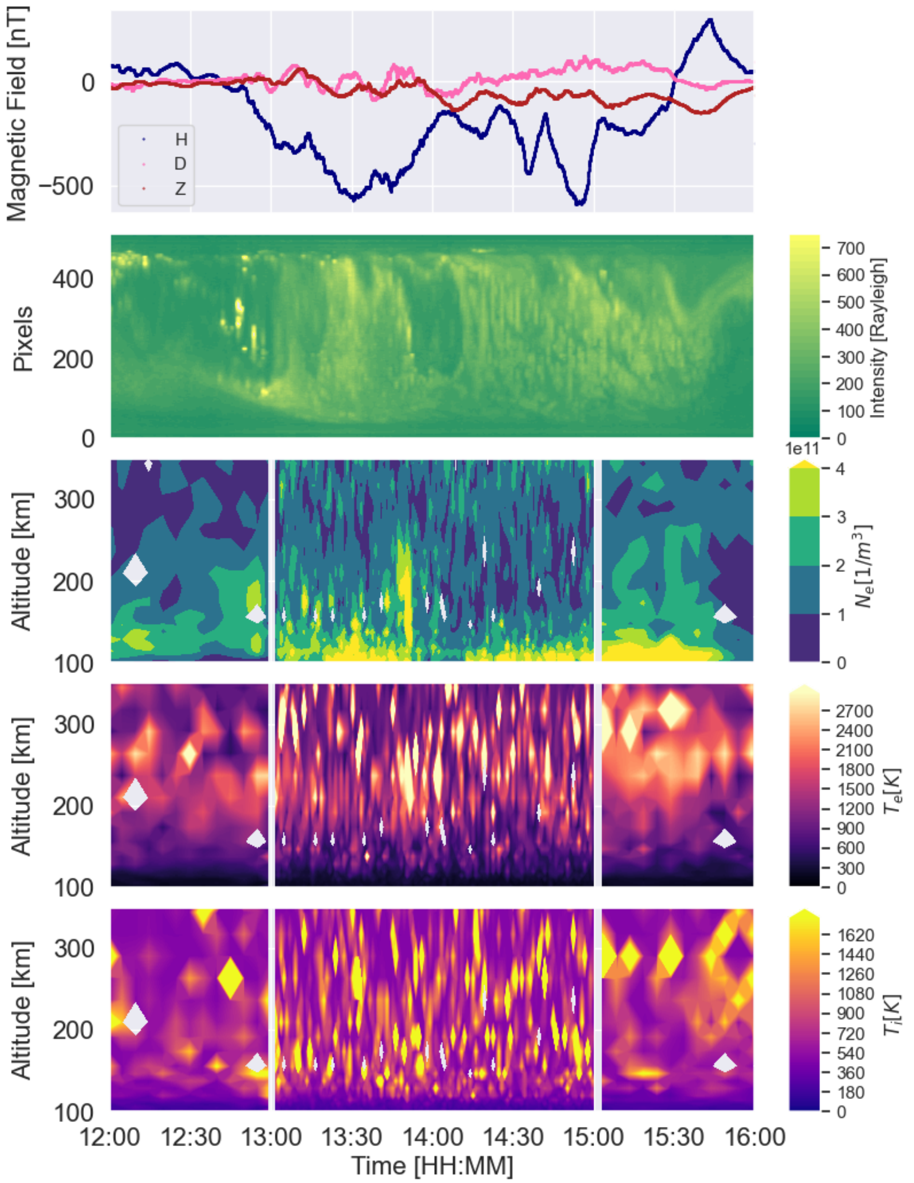

PFISR is an invaluable instrument for M-I-T coupling research.

- PFISR provides versatile data products that can be used for input, analysis, and validation.

- PFISR can help identify various meso-scale phenomena linked to substorms, travelling convection vortices, and meteors to name a few.

- Situated at PFRR alongside a suite of complementary instruments such as magnetometers, lidars, ASIs, and SDIs, PFISR also provides contextual measurements for investigations of high-latitude upper atmosphere.

- Driven by the current research directive to enhance high-resolution forecasting and modeling, PFISR is crucial enabling studies of meso- and small-scale electrodynamics; its continued operations are necessary to sustain progress in this domain.

Thank you!
Questions?

Special thanks to, Shasha Zou, Aaron Ridley, James Slavin, Olga Verkhoglyadova, Mike Hartinger, Xing Meng, Jeremiah Johnson, Steve Kaeppler, Katrina Bossert, Xueling Shi, Leslie Lamarche, Asti Bhatt, Ashton Reimer, Roger Varney, Josh Semeter, Pablo Reyes, Chen Wu, Nick Bartell, Tomoko Matsuo, and Don Hampton.

Back-Up Slides

ML tools can help process large visual data sets.

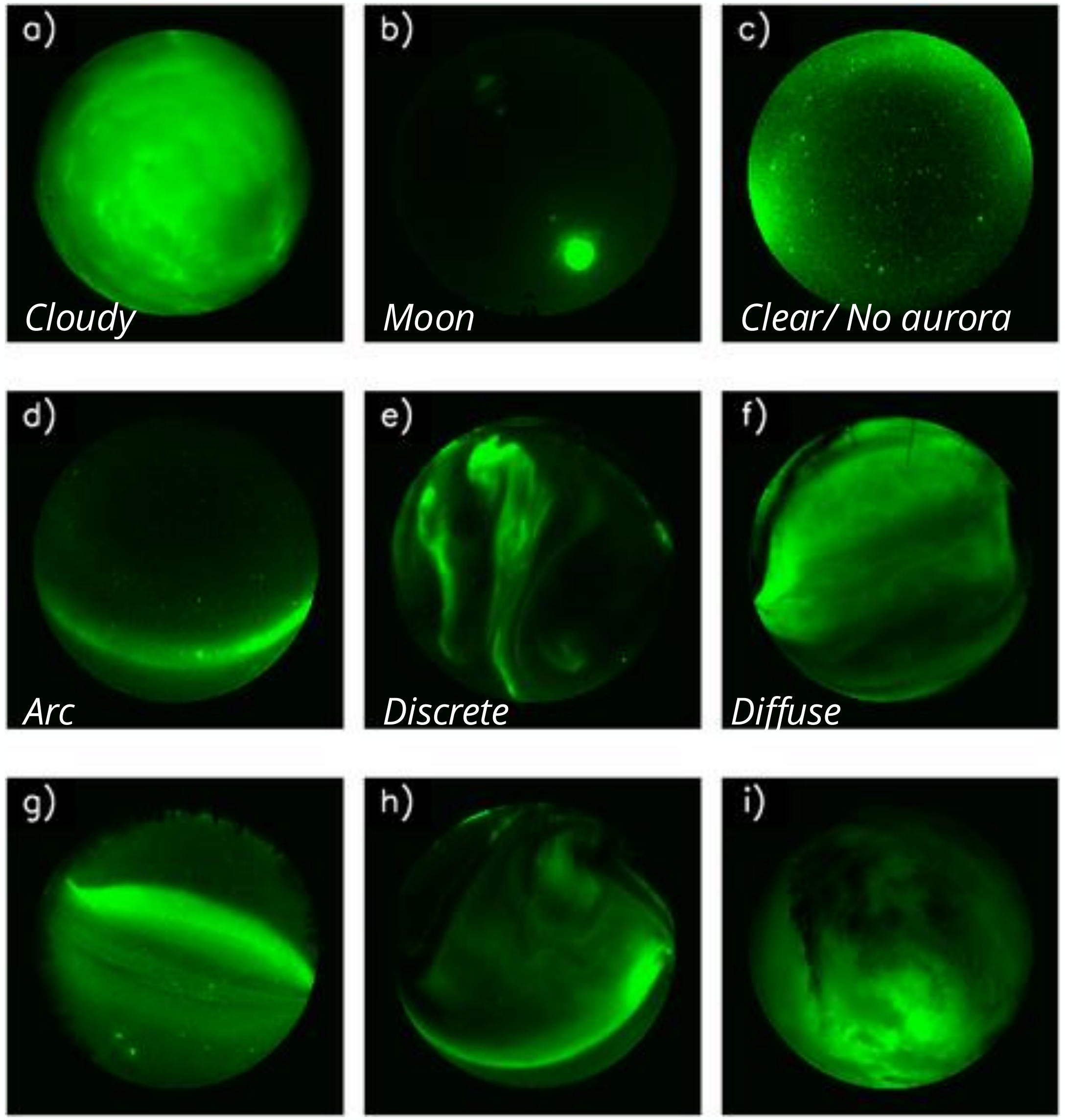

Clausen and Nickisch, 2018

- 23 imagers across North America.
- Over 3 billion images: not curated or labelled, unbalanced, ambiguous.
- Opportunities for broad statistical studies and developing predictive models.

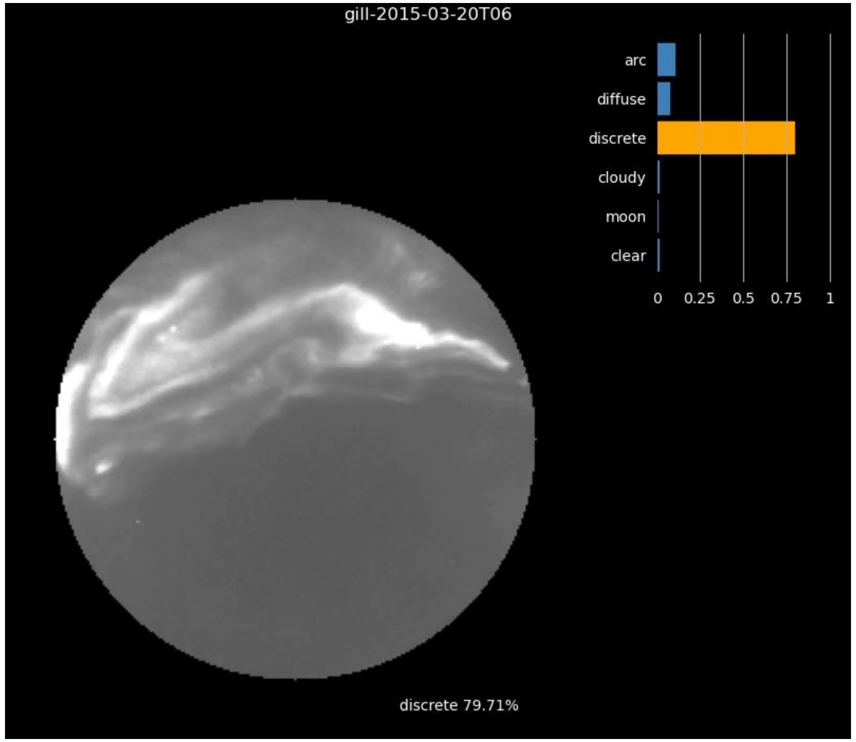

- Adapted a Simple Framework for Contrastive Learning of Visual Representations (SimCLR).

- Achieved over 95% accuracy on the OATH data set.

Two-stage training model applied to OATH data set.

Stage-1: Self-Supervised Representation Learning

1. For all data in minibatch, form all possible pairs of views (transformed data) (x_i, x_j). Note that this includes different views of the *same* (single) input image
2. Pass pairs (x_i, x_j) through encoder -> projection head and calculate *cosine similarity* of outputs (z_i, z_j)
3. If (x_i, x_j) are different views of the same (single) input image, they form a positive example. If they are produced from different input images, they form a negative example. Training objective is simple **binary** classification: positive example or negative example?
4. Post-training, discard projection head and extract learned representations $\boldsymbol{h}$

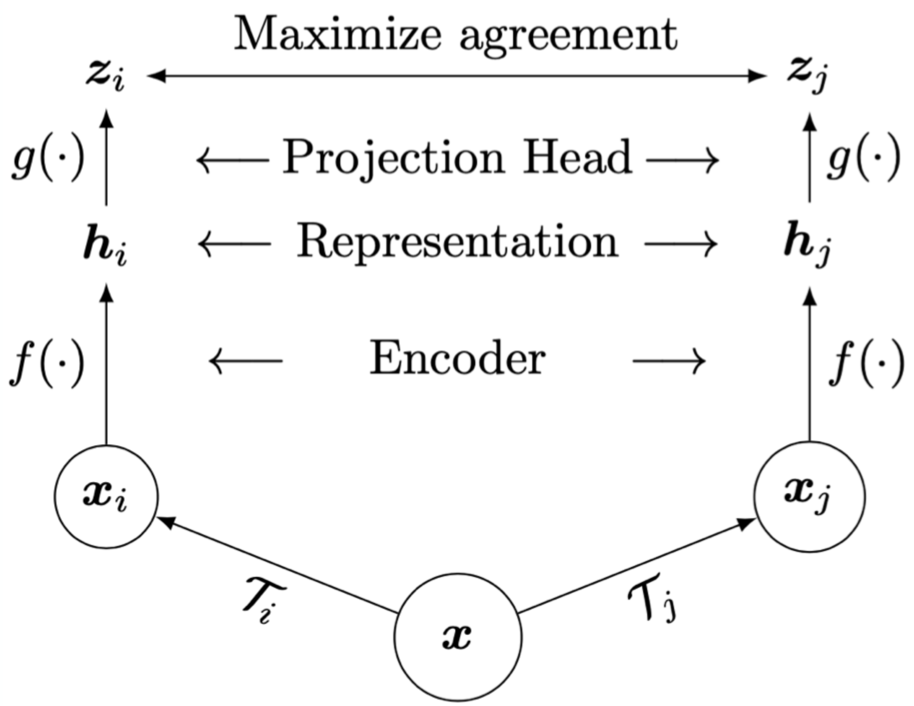

Two-stage training model applied to OATH data set.

Stage-2: Semi-Supervised Training

1. Using a small amount of annotated data (Oslo Aurora THEMIS dataset, ~6000 images), first train a classifier to a sufficient level of performance.
2. Continue training, and periodically make predictions on unlabeled data.
3. Treat high-confidence predictions as ground-truth annotations and add these data to training dataset.
4. Repeat.

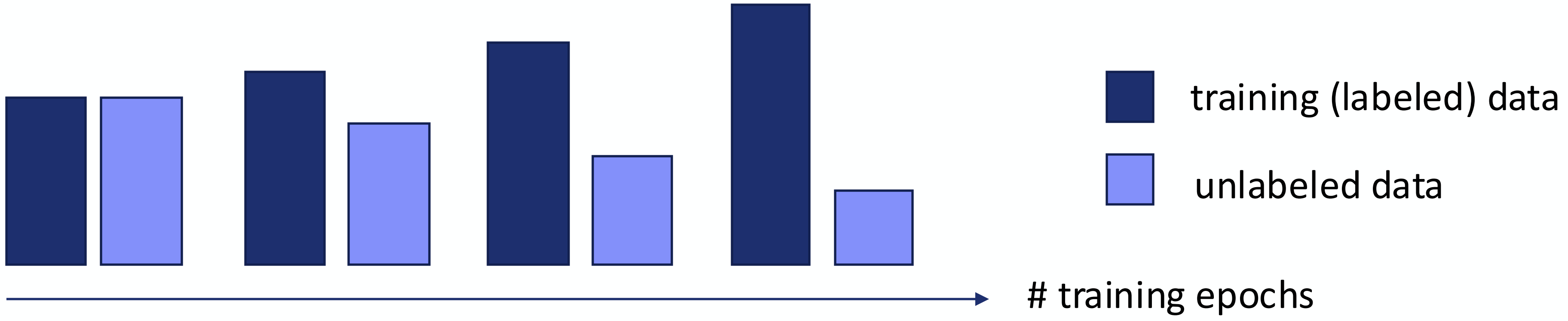

Applying SimCLR to OATH dataset yields to high accuracy classification.

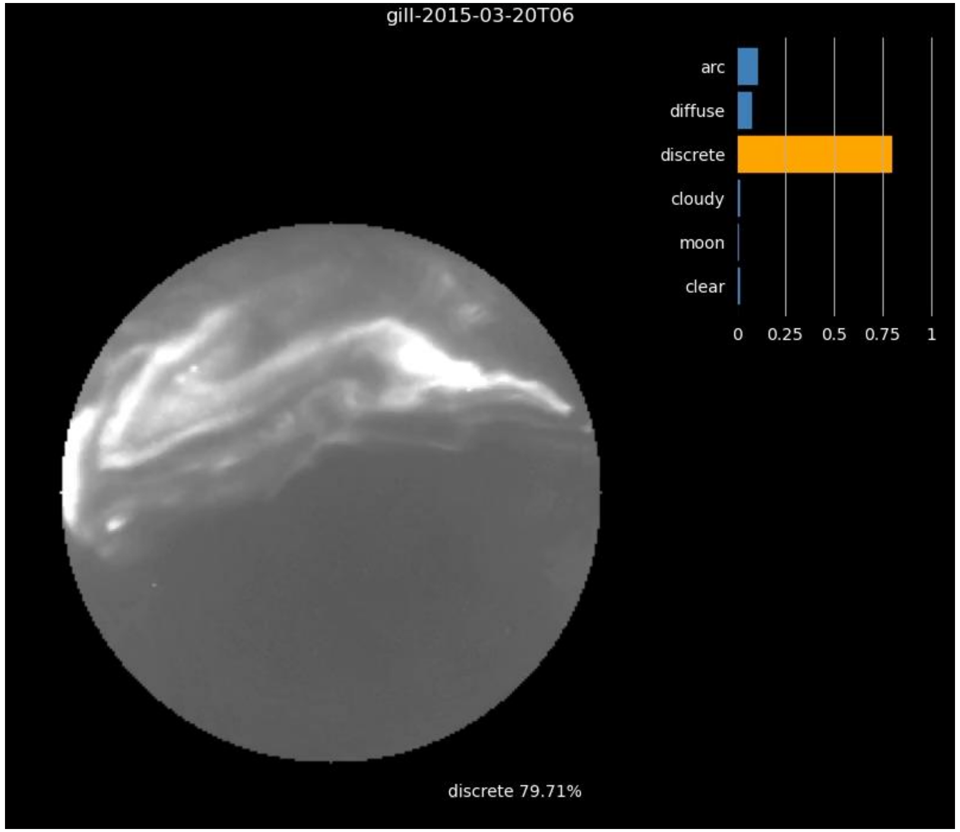

Model Hyperparameters:

- Self-supervision with ~1e6 THEMIS ASIs
- ResNet18 encoder (not pretrained)
- 60 epochs of self-supervised training, batch size 128, Adam optimizer, cosine annealed learning rate
- Classifier training and finetuning with ~6000 OATH images
- 100 epochs of classifier training, batch size 128, Adam optimizer, scheduled learning rate changes

On OATH data set, preliminary SimCLR accuracy was **90.9%.**

Model	Params.	Top–1 Accuracy (%)	Std.	Precision	Recall	F1–Score
Ridge + Inception (pretrained) [12]	43m	81.7	0.1	83.0*	84.3*	83.6*
ResNet18 (pretrained, supervised)	12m	84.7	0.7	85.6	85.2	85.3
SimCLR	12m	**90.9**	0.7	**91.6**	**91.5**	**91.5**

Johnson et al., 2021

How to increase the model accuracy further?

Classification of the THEMIS ASI Dataset with the Semi-Supervised Model

- Applied to all data between 2008-2022.
- Figure displays over 706 million labels after confidence threshold applied.
- 4 to 5 orders of magnitude higher than other classification studies in the literature.
- Conducted statistical studies between upstream solar wind data, labels, and ground magnetic field signatures.

Johnson et al., in review

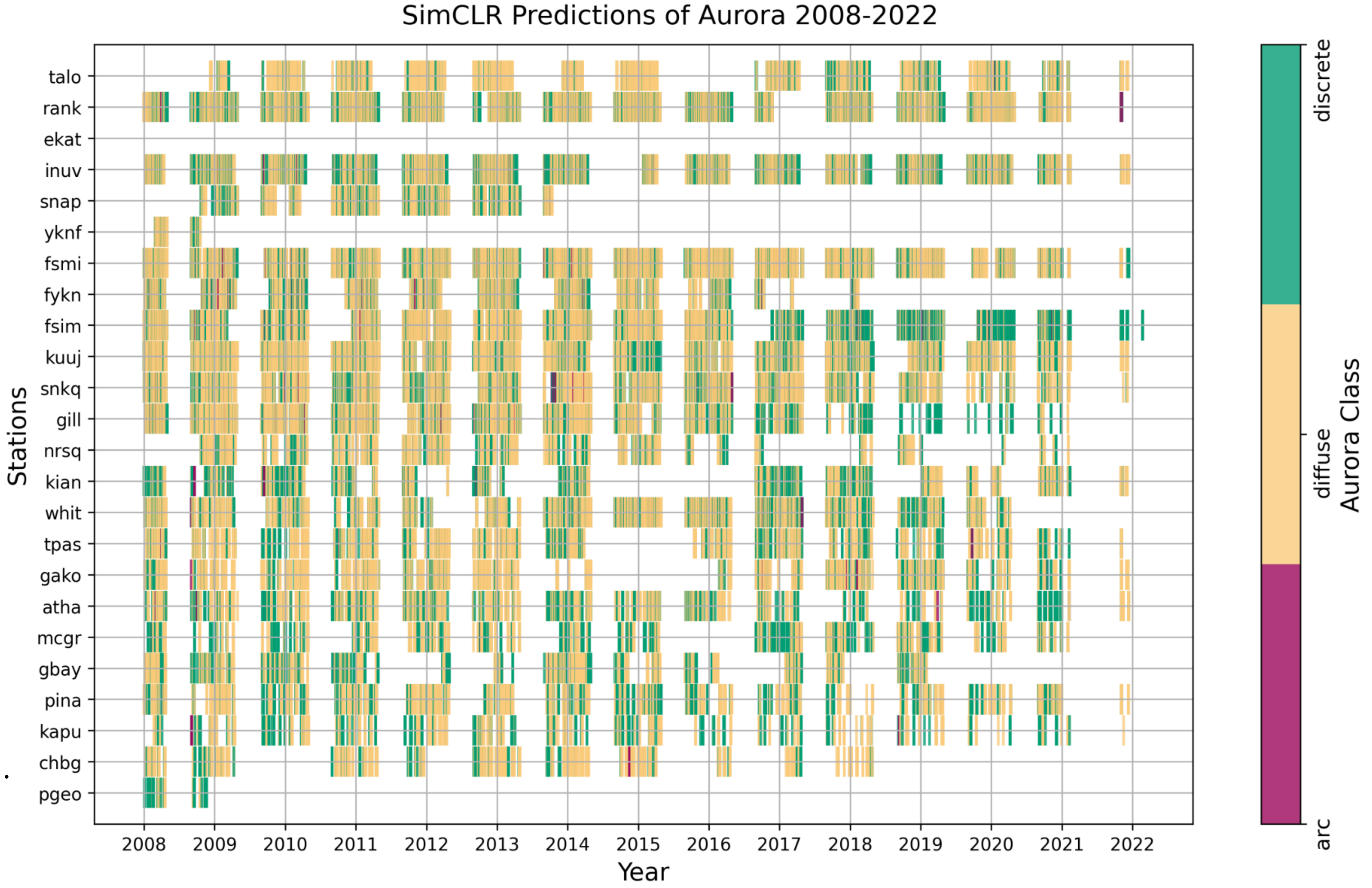

Heat Transfer Rate from Ions to Neutrals

$$\frac{dT_n}{dt} = \frac{1}{\rho C_p}\left[\left(\sum_{\text{ions}} \frac{n_n m_n \upsilon_{ni}}{(m_i + m_n)}\left[\underbrace{3k(T_i - T_n)}_{\text{Collisional heat transfer rate}} + \underbrace{m_i(u_i - u_n)^2}_{\text{Frictional heat transfer rate}}\right]\right) \underbrace{- \frac{\partial}{\partial z}\left(\lambda_n \frac{\partial T_n}{\partial z}\right)}_{\text{Vertical heat conduction rate}}\right]$$